



J. Houghton, C., & J. Weinberg, E. (2002). Multicloud solutions with massless and massive monopoles. *Physical Review D: Particles and Fields*, 66(12), [125002]. <https://doi.org/10.1103/PhysRevD.66.125002>

Early version, also known as pre-print

Link to published version (if available):
[10.1103/PhysRevD.66.125002](https://doi.org/10.1103/PhysRevD.66.125002)

[Link to publication record in Explore Bristol Research](#)
PDF-document

Conor J. Houghton and Erick J. Weinberg: Multicloud solutions with massless and massive monopoles
Phys. Rev. D 66, 125002 – Published 11 December 2002
Copyright 2002 by the American Physical Society.

University of Bristol - Explore Bristol Research

General rights

This document is made available in accordance with publisher policies. Please cite only the published version using the reference above. Full terms of use are available:
<http://www.bristol.ac.uk/pure/about/ebr-terms>

Multicloud solutions with massless and massive monopoles

Conor J. Houghton^{a*} and Erick J. Weinberg^{b†}

^a*School of Mathematics, Trinity College, Dublin 2, Ireland*

^b*Department of Physics, Columbia University, New York, NY 10027*

Abstract

Certain spontaneously broken gauge theories contain massless magnetic monopoles. These are realized classically as clouds of non-Abelian fields surrounding one or more massive monopoles. In order to gain a better understanding of these clouds, we study BPS solutions with four massive and six massless monopoles in an $SU(6)$ gauge theory. We develop an algebraic procedure, based on the Nahm construction, that relates these solutions to previously known examples. Explicit implementation of this procedure for a number of limiting cases reveals that the six massless monopoles condense into four distinct clouds, of two different types. By analyzing these limiting solutions, we clarify the correspondence between clouds and massless monopoles, and infer a set of rules that describe the conditions under which a finite size cloud can be formed. Finally, we identify the parameters entering the general solution and describe their physical significance.

*Email address: houghton@maths.tcd.ie

†Email address: ejw@phys.columbia.edu

I. INTRODUCTION

Magnetic monopole soliton solutions arise in certain spontaneously broken gauge theories. After quantization, these give rise to magnetically charged particles that can be regarded as the counterparts of the electrically charged elementary particles of the theory. Indeed, it is believed that in certain supersymmetric theories there is an exact duality symmetry [1] relating these two classes of particles.

An interesting new feature arises if the unbroken gauge group contains a non-Abelian subgroup. The massless gauge bosons of this subgroup transform nontrivially under the gauge group, and thus carry an “electric charge”. Duality then predicts that these should have massless magnetically-charged counterparts. These cannot be realized as isolated classical solutions. However, evidence for their existence has been found by analyzing certain multimonopole solutions [2]. These solutions can be viewed as containing a “cloud” of non-Abelian fields that surrounds one or more massive monopoles. Evidently, this cloud is the manifestation of the massless monopole.

The previously known solutions of this type either have a single cloud that generally, although not always, corresponds to a single massless monopole, or else have two independent clouds. In this paper, we obtain a new class of solutions that has a much richer structure. By analyzing these, we are able to gain further insight into the nature of the massless monopoles.

To explain this in more detail, we need to establish some conventions. Throughout, we consider a gauge theory with an adjoint representation Higgs field Φ and restrict ourselves to BPS solutions [3,4] obeying the Bogomolny equation

$$D_i\Phi = B_i \equiv \frac{1}{2}\epsilon_{ijk}F_{jk}. \quad (1.1)$$

Except in this introduction, we will assume that the fields have been rescaled so as to set the gauge coupling e to unity.

Both Φ and the gauge potential A_i can be regarded as elements of the Lie algebra. Recall that a basis for this algebra can be chosen to be a set of r commuting generators H_i that form the Cartan subalgebra, together with raising and lowering operators E_{α} associated with the roots. By an appropriate gauge transformation, the Higgs expectation value can be chosen to be of the form

$$\Phi_0 = \mathbf{h} \cdot \mathbf{H}. \quad (1.2)$$

If the r -component vector \mathbf{h} has nonzero inner products with all of the roots, the symmetry breaking is maximal and the unbroken symmetry group is the maximal torus $U(1)^r$. If, however, some roots are orthogonal to \mathbf{h} , then there is a non-Abelian unbroken subgroup

K of rank $r' < r$. The roots of K are precisely the roots that are orthogonal to \mathbf{h} and the symmetry is broken to $K \times U(1)^{r-r'}$.

A basis for the root lattice is given by a set of r simple roots β_a . We require that these satisfy $\mathbf{h} \cdot \beta_a \geq 0$. This determines the set uniquely in the case of maximal symmetry breaking, but only up to a Weyl transformation when there is nonmaximal breaking.

At large distances, the magnetic field must commute with the Higgs field. Hence, in a direction where the asymptotic Higgs field is of the form of Eq. (1.2), the magnetic field can be put in the form

$$B_i = \frac{Q_M \hat{r}_i}{r^2} + O(r^{-3}) \quad (1.3)$$

where the magnetic charge Q_M is an element of the Cartan sub-algebra. The topological quantization condition requires that [5]

$$Q_M = \frac{4\pi}{e} \sum_{a=1}^r k_a \frac{\beta_a}{\beta_a^2} \cdot \mathbf{H} \quad (1.4)$$

with the k_a all being integers; for self-dual BPS solutions these will all be positive.

In the case of maximal symmetry breaking, the simple roots can be used to construct a set of r fundamental monopoles. These are obtained by embedding the unit $SU(2)$ monopole (appropriately rescaled) in the $SU(2)$ subgroup associated with each of the β_a . The β_a -monopole thus defined has mass $m_a = (4\pi/e^2)\mathbf{h} \cdot \beta_a$ and the radius of its core region is roughly $1/(e^2 m_a)$. It carries one unit of the topological charge k_a , while the remaining k_b all vanish. Zero-mode analysis shows that this solution has four zero modes, requiring the introduction of four collective coordinates. Three of these specify the position of the monopole, while the fourth is a $U(1)$ phase; dyonic solutions can be obtained by allowing this phase to become time-dependent. An arbitrary static BPS solution can be interpreted as being composed of a collection of these fundamental monopoles, with the k_a specifying the number of each type [6]. In particular, the energy is the sum of the component masses while the number of zero modes is $4 \sum k_a$.

The case of non-Abelian symmetry breaking can be obtained by varying the Higgs expectation value so that \mathbf{h} is orthogonal to some of the β_a ; we will often write γ_a to indicate the latter. The BPS mass formula implies that the fundamental monopoles corresponding to the γ_a should be massless. Actually, there is no classical solution corresponding to these monopoles, since the prescription for embedding the $SU(2)$ monopole gives a trivial vacuum solution in this limit. Nevertheless, the formulas for the mass and counting of zero modes in terms of the k_a remain valid,¹ suggesting that the interpretation of higher charged solutions

¹To maintain the validity of the zero-mode counting, as well as to avoid a number of pathologies

in terms of component fundamental monopoles should be retained [8].

Some insight can be obtained by considering specific examples. The simplest [9] arises in the context of $SO(5)$ broken to $SU(2)\times U(1)$. There are two species of fundamental monopoles, one massive and one massless. The solutions in which we are interested contain one of each; we will refer to it as a $(1,[1])$ solution, with the square brackets indicating that the corresponding monopole is massless. Because these solutions turn out to be spherically symmetric, the BPS equations can be reduced to a set of ordinary differential equations that can be explicitly solved in terms of rational and hyperbolic functions. Examining the solutions, one finds a massive core of fixed size that is surrounded by a spherical cloud of radius a . Inside the cloud there is a Coulomb magnetic field, with both Abelian and non-Abelian components, that corresponds to the magnetic charge of the massive fundamental monopole. Outside the cloud, the non-Abelian components of the magnetic field fall off as $1/r^3$, leaving the purely Abelian Coulomb field appropriate to the sum of the two component monopoles. The energy of the solution is independent of the cloud radius a , which can take on any positive real value.

In these solutions, the massive monopole is evident and has a well defined position. The massless monopole is clearly associated with the cloud, but it is less clear how to define its position. To illustrate this, consider an arbitrary $(1,1)$ solution in the theory with $SO(5)$ maximally broken to $U(1)\times U(1)$. If the direction of the Higgs expectation value is varied continuously until the second fundamental monopole becomes massless, this solution approaches one of the $(1,[1])$ solutions. The separation of the massive monopoles in the initial solution becomes the cloud parameter in the final solution. However, the direction of the separation vector has no effect on the final solution.

More complex solutions have been studied with the aid of the Nahm construction, which we describe below. Two examples, both containing one massless and two massive monopoles, will play an important role in our considerations. One is the $(1,[1],1)$ solution [10] for the case of $SU(4)$ broken to $U(1)\times SU(2)\times U(1)$, and the other is the $(2,[1])$ Dancer solution [11,12] for $SU(3)$ broken to $SU(2)\times U(1)$. In both cases, the massless monopole is manifested as a cloud that encloses both of the massive monopoles. Inside the cloud, one finds the Abelian and non-Abelian Coulomb magnetic fields appropriate to the charges and positions of the massive monopoles. Outside the cloud only the Abelian component survives. As in the

[7] associated with non-Abelian magnetic charges, we will assume that the total magnetic charge is Abelian. This is not a significant restriction, in that any solution with non-Abelian magnetic charge can be viewed as a purely Abelian one in which the compensating monopoles are located arbitrarily far away.

SO(5) example, the cloud is parameterized by a single collective coordinate that determines its size. [An Sp(4) solution with one massless and two massive monopoles is described in Ref. [13].]

In order to understand better the nature of these clouds, it would be helpful to have some examples of solutions with two or more distinct clouds, or at least with clouds that had more structure. It might be expected that such solutions could be obtained simply by adding additional massless monopoles. This is not necessarily so. For example, the $(1, [1], 1)$ solutions in SU(4) can be readily generalized [10] to $(1, [1], \dots, [1], 1)$ solutions for SU(N) broken to $U(1) \times SU(N-2) \times U(1)$. However, although the generalized solutions have $N-3$ massless monopoles, the spacetime fields display only a single one-parameter ellipsoidal cloud, no matter what the value of N . In fact, the solutions are simply embeddings of the SU(4) solution into the larger group.

One example with two non-Abelian clouds is the $([1], 2, [1])$ solution in SU(4) broken to $U(1) \times SU(N-2) \times U(1)$ [14,15]. However, the two clouds do not interact directly and the structure is no richer than the $(2, [1])$ Dancer solution.

A more promising choice, on which we will focus in this paper, is the family of $(2, [2], \dots, [2], 2)$ solutions for SU(N) broken to $U(1) \times SU(N-2) \times U(1)$. For certain special choices of parameters, these essentially reduce to a pair of widely separated $(1, [1], \dots, [1], 1)$ solutions. In general, however, these solutions are considerably more complex. At the same time, they are reasonably tractable.

Let us expand upon this last point. Except for a few symmetric solutions, such as the SU(2) unit monopole and the SO(5) solution $(1, [1])$ solution discussed above, the Bogomolny equation is too difficult to solve directly. Instead, it is easier to use a construction due to Nahm [16]. This Nahm construction has three distinct steps. In the first, one solves the Nahm equation, which is a set of nonlinear ordinary differential equations for a set of matrices $T_i(s)$. These Nahm data, as they are called, then specify a linear differential equation, the construction equation. Finally, the spacetime fields are obtained by integration of quantities that are bilinear in the solutions of the construction equations.

This construction can be carried out explicitly for both the $(1, [1], 1)$ SU(4) solution noted above and the analogous $(1, 1, 1)$ solution in the maximally broken theory [10]. For the $(2, [1])$ Dancer solution, the Nahm equation can be solved, yielding data that are expressed in terms of elliptic functions. Except for special cases, however, the resulting construction equation can only be solved asymptotically, allowing one to obtain approximations to the spacetime fields that are valid far from the massive monopole cores.

The remainder of the paper is organized as follows. In Sec. II, we give an overview of the Nahm construction and establish some conventions. Next, in Sec. III, we discuss the param-

eters entering the various solutions we will be considering. We also describe how to solve the Nahm equation to obtain the data for the $SU(N)$ $(1, [1], \dots, [1], 1)$ solution, the $SU(3)$ Dancer solution, and, finally, the $(2, [2], \dots, [2], 2)$ solutions that will be our main focus. In Sec. IV we describe how the $(k, [k], \dots, [k], k)$ for $SU(N)$ can be obtained algebraically from a knowledge of the $(k, [k-1], [k-2], \dots, [1])$ solutions of $SU(k+1)$. As an example of this, we show how the $(1, [1], \dots, [1], 1)$ solutions can be easily recovered. For the case $k=2$, which is our primary interest, we need some special limits of the Dancer solution; these are described in Sec. V. In Sec. VI, we use these Dancer results in the construction of Sec. IV to obtain $(2, [2], \dots, [2], 2)$ solutions for a variety of limiting cases. We describe the nature of the clouds in each. In Sec. VII we use these solutions to abstract some general rules describing how clouds form about massive monopoles. This clarifies the relationship between clouds and massless monopoles. Finally, in Sec. VIII, we summarize our results and add some concluding remarks.

II. THE NAHM CONSTRUCTION

The Bogomolny equation is reciprocal to the Nahm equation. This means that the solutions of the Bogomolny equation may be constructed from the solutions of the Nahm equation and visa versa. Furthermore, the moduli space of solutions to the Bogomolny equation is isometric to the moduli space of solutions to the Nahm equations. The reciprocal relationship is similar to the relationship between the self-dual Yang-Mills equations and the ADHM data [17].

A. Nahm data for $SU(2)$ monopoles

The Nahm equation is an equation for a quadruple of Hermitian matrix functions of a single variable s :

$$\frac{dT_i}{ds} + i[T_0, T_i] = -\frac{i}{2}\epsilon_{ijk}[T_j, T_k]. \quad (2.1)$$

Solutions of the Nahm equations are called Nahm data. The size of the matrices and the boundary conditions that they satisfy determine the monopole charge in the reciprocal Bogomolny problem. For an $SU(2)$ solution with k monopoles of mass m , the variable s lies in the interval $(-m/2, m/2)$ and the data are $k \times k$ matrices. The matrices T_1 , T_2 and T_3 are required to have simple poles at $s = \pm m/2$, while T_0 must be finite at these end points. By expanding

$$T_i(s) = -\frac{1}{s \mp m/2} R_i^\pm + O(1) \quad (2.2)$$

near $s = \pm m/2$ and substituting back into the Nahm equations, it is easy to see that the matrix residues R_i^\pm satisfy the $SU(2)$ commutation relations

$$[R_i^\pm, R_j^\pm] = i\epsilon_{ijk}R_k^\pm. \quad (2.3)$$

It is required as a boundary condition that the matrix residues form an irreducible k -dimensional representation of $SU(2)$. The case $k = 1$ is special, because the one-dimensional representation of $SU(2)$ is trivial and in fact, for $k = 1$ there are no poles at the end points. The role played by the boundary condition will become clear shortly, when we discuss the construction of monopole fields. Before doing this, it is useful to examine the symmetry groups acting on the Nahm data.

There is an $SU(k)$ group action on the data given by

$$\begin{aligned} T_i &\rightarrow gT_i g^{-1} \\ T_0 &\rightarrow gT_0 g^{-1} + i\frac{dg}{ds}g^{-1} \end{aligned} \quad (2.4)$$

where g is an $SU(k)$ function of s . This action does not affect the monopole fields that are constructed from the Nahm data. This action is usually referred to as the gauge action. In the $SU(2)$ case, this action is customarily fixed by requiring $T_0 = 0$ and specifying the matrix residues.

There are two further group actions. There is an $SU(2)$ action which rotates (T_1, T_2, T_3) as a three-vector:

$$T_i \rightarrow R_{ij}T_j \quad (2.5)$$

and there is a \mathbf{R}^3 action which translates the traces:

$$T_i \rightarrow T_i + \lambda_i I_k. \quad (2.6)$$

These actions correspond to rotation and translation of the monopole fields themselves. Of course, if the gauge has been fixed by specifying the residues then the rotation action must include a compensating gauge transformation.

The spacetime gauge and Higgs fields are obtained from the Nahm data by first solving the construction equation,

$$\Delta^\dagger v = \left(-\frac{d}{ds} - T_i \otimes \sigma_i + I_k \otimes r_i \sigma_i \right) v(s; \mathbf{r}) = 0 \quad (2.7)$$

for the $2k$ -vector function v , which we will refer to as the construction data. (To simplify our notation, we will often not explicitly show the \mathbf{r} dependence of v .) An inner product between any two such vector functions v and v' is given by

$$\langle v|v' \rangle = \int_{-m/2}^{m/2} v^\dagger v' ds. \quad (2.8)$$

With this inner product, there are precisely two linearly independent normalizable solutions to Eq. (2.7). We choose these to be orthonormal.

It is easy to see why there are only two solutions. Near $s = m/2$

$$\Delta^\dagger \approx - \left[\frac{d}{ds} - \frac{1}{s - m/2} R_i \otimes \sigma_i \right] \quad (2.9)$$

where (R_1, R_2, R_3) are irreducible $k \times k$ representation matrices for $SU(2)$. $R_i \otimes \sigma_i$ has two eigenvalues: $(k - 1)/2$ with degeneracy $k + 1$ and $-(k + 1)/2$ with degeneracy $k - 1$. This can be shown by choosing an explicit basis and calculating directly. However, it is useful to examine the elegant group theoretical argument, familiar from the addition of angular momenta, that is given in [18]. If (R_1, R_2, R_3) is a representation of $SU(2)$, then $C = \sum R_i^2$ is the Casimir operator. For the k -dimensional irreducible representation, this is $C_{\mathbf{k}} = \frac{1}{4}(k + 1)(k - 1)I_k$. It is possible to rewrite $R_i \otimes \sigma_i$ in terms of Casimir operators. Because $\mathbf{k} \otimes \mathbf{2} = (\mathbf{k} + \mathbf{1}) \oplus (\mathbf{k} - \mathbf{1})$,

$$C_{(\mathbf{k}+\mathbf{1})\oplus(\mathbf{k}-\mathbf{1})} = (R_i \otimes I_2 + I_k \otimes \frac{1}{2}\sigma_i)^2 = C_{\mathbf{k}} \otimes I_2 + R_i \otimes \sigma_i + I_k \otimes C_{\mathbf{2}} \quad (2.10)$$

or,

$$\begin{aligned} R_i \otimes \sigma_i &= C_{(\mathbf{k}+\mathbf{1})\oplus(\mathbf{k}-\mathbf{1})} - C_{\mathbf{k}} \otimes I_2 - I_k \otimes C_{\mathbf{2}} \\ &= C_{(\mathbf{k}+\mathbf{1})\oplus(\mathbf{k}-\mathbf{1})} - \frac{(k^2 + 2)}{4} I_{2k} \\ &= \frac{(k - 1)}{2} I_{k+1} \oplus \frac{(-k - 1)}{2} I_{k-1}. \end{aligned} \quad (2.11)$$

Thus, a vector in $\mathbf{k} + \mathbf{1}$ is an eigenvector of $R_i \otimes \sigma_i$ with eigenvalue $(k - 1)/2$ and a vector in $\mathbf{k} - \mathbf{1}$ is an eigenvector with eigenvalue $-(k + 1)/2$.

In order to be normalizable, v must lie in the eigenspace with eigenvalue $(k - 1)/2$ and so it must be perpendicular to the $k - 1$ vectors in $\mathbf{k} + \mathbf{1}$. This gives $k - 1$ conditions. The pole at $s = -m/2$ gives another $k - 1$ conditions in the same way, and so there are two normalizable solutions. If v_1 and v_2 are an orthonormal basis for these solutions, then the fields are given by

$$\begin{aligned} \Phi_{ab} &= \langle v_a | s | v_b \rangle = \int_{-m/2}^{m/2} s v_a^\dagger v_b ds \\ (A_i)_{ab} &= -i \langle v_a | \partial_i | v_b \rangle = -i \int_{-m/2}^{m/2} v_a^\dagger \partial_i v_b ds. \end{aligned} \quad (2.12)$$

These fields can be shown to satisfy the Bogomolny equations. This follows from the fact that the Nahm equations imply that $\Delta \Delta^\dagger$ commutes with $I_k \otimes \sigma_i$. Without dwelling too

much on the details, which can be found in [19], the argument runs as follows. By explicit calculation

$$\left(\frac{1}{2}\epsilon_{ijk}F_{jk}\right)_{ab} = -i\epsilon_{ijk} \int \int \partial_j v_a^\dagger(s) [I_{2k}\delta(s-s') - v_c(s)v_c(s')^\dagger] \partial_k v_b(s') ds ds'. \quad (2.13)$$

Now, the operator $\int [I_{2k}\delta(s-s') - v_c(s)v_c(s')^\dagger] ds'$ is a projection operator that projects onto the null space of Δ^\dagger . This means that it can be replaced by the projection operator $\int \Delta(\Delta^\dagger\Delta)^{-1}\Delta^\dagger ds'$ and so

$$\left(\frac{1}{2}\epsilon_{ijk}F_{jk}\right)_{ab} = -i\epsilon_{ijk} \int \int \partial_j v_a^\dagger(s) \Delta(\Delta^\dagger\Delta)^{-1}\Delta^\dagger \partial_k v_b(s') ds' ds. \quad (2.14)$$

The construction equation implies that $\Delta^\dagger\partial_i v = -I_k \otimes \sigma_i v$. Hence, using $[\Delta\Delta^\dagger, I_k \otimes \sigma_i] = 0$, we obtain

$$\left(\frac{1}{2}\epsilon_{ijk}F_{jk}\right)_{ab} = 2 \int \int v_a^\dagger(s) I_k \otimes \sigma_i (\Delta^\dagger\Delta)^{-1} v_b(s') ds' ds. \quad (2.15)$$

This is half of the argument. The other half of the argument shows that $(D_i\Phi)_{ab}$ also equals the right hand side of the above equation. This half of the argument is very similar to the one just given, the main difference is that it uses $\Delta^\dagger s v = -v$ as well as $\Delta^\dagger\partial_i v = -I_k \otimes \sigma_i v$.

It is also useful to describe how the matrix size determines the monopole charge. We will follow the proof given in [18]. For large r , Δ^\dagger is approximated by

$$\tilde{\Delta}^\dagger = -\frac{d}{ds} + \left(\frac{1}{s-m/2} + \frac{1}{s+m/2}\right) R_i \otimes \sigma_i + I_k \otimes x_i \sigma_i. \quad (2.16)$$

$\tilde{\Delta}^\dagger$ differs from Δ^\dagger in two ways. Firstly, the Nahm data have been approximated by their behavior near the pole. It can be shown that this affects the calculation of Φ at order $1/r^2$. The other difference is that the matrix residues are assumed to be the same at each end. In fact, while they are both required to form the same representation, they could differ by a unitary conjugation. This subtlety is not important since it corresponds to an s -dependent unitary transformation of v and does not affect the fields.

The eigenvalues of

$$\left(\frac{1}{s-m/2} + \frac{1}{s+m/2}\right) R_i \otimes \sigma_i + I_k \otimes x_i \sigma_i \quad (2.17)$$

are independent of direction and depend only on r . In fact, the large- r fields calculated using $\tilde{\Delta}$ are spherically symmetric and so we can take $\mathbf{r} = (0, 0, r)$. This means that $I_k \otimes x_i \sigma_i$ commutes with $R_3 \otimes \sigma_3$. Furthermore, $R_3 \otimes \sigma_3$ has a unique eigenvector of eigenvalue k and another of eigenvalue $-k$ lying in the $\mathbf{k} + \mathbf{1}$ of $\mathbf{k} \otimes \mathbf{2} = (\mathbf{k} + \mathbf{1}) \oplus (\mathbf{k} - \mathbf{1})$. These eigenvalues are exceptional, in that all the other eigenspaces are two-dimensional, being spanned by an

eigenvector from $\mathbf{k} + \mathbf{1}$ and an eigenvector from $\mathbf{k} - \mathbf{1}$. Since the $\pm k$ eigenvectors are in $\mathbf{k} + \mathbf{1}$, we know how they are acted on by $R_i \otimes \sigma_i$: both of them have eigenvalue $(1 - k)/2$. Since $(\mathbf{1}_k \otimes x_i \sigma_i)^2 = r^2 \mathbf{I}_{2k}$, we also know how they are acted on by $\mathbf{I}_k \otimes x_i \sigma_i$: they have eigenvalues r and $-r$. Let us denote the two eigenvectors v_+ and v_- respectively.

Now, if we substitute $v(s) = g_\pm(s) v_\pm$ into the approximate construction equation $\tilde{\Delta}^\dagger v = 0$, we get

$$\frac{dg_\pm}{ds} + \frac{k-1}{2} \left(\frac{1}{s-m/2} + \frac{1}{s+m/2} \right) g_\pm \pm r g_\pm = 0, \quad (2.18)$$

which is solved by

$$g_\pm = \left(s^2 - \frac{m^2}{4} \right)^{(k-1)/2} e^{\pm rs}. \quad (2.19)$$

Because v_\pm are pointwise orthogonal, we need only consider the diagonal components of $\tilde{\Phi}$. For large r , the exponential in g_+ means that the value of any integral of a polynomial times g_+^2 is dominated by the value of the integrand near $m/2$. This allow us to approximate

$$\int_{-m/2}^{m/2} g_+^2 ds = \int_{-m/2}^{m/2} \left(s^2 - \frac{m^2}{4} \right)^{k-1} e^{2rs} ds \approx e^{mr} \int_{-\infty}^0 e^{2ru} u^{k-1} (m+u)^{k-1} du \quad (2.20)$$

and

$$\int_{-m/2}^{m/2} s g_+^2 ds = \int_{-m/2}^{m/2} s \left(s^2 - \frac{m^2}{4} \right)^{k-1} e^{2rs} ds \approx e^{mr} \int_{-\infty}^0 e^{2ru} u^{k-1} (m+u)^{k-1} \left(\frac{m}{2} + u \right) du. \quad (2.21)$$

We can then integrate by parts and show that

$$\tilde{\Phi}_{11} = \frac{\int_{-m/2}^{m/2} s g_+^2 ds}{\int_{-m/2}^{m/2} g_+^2 ds} = \frac{m}{2} - \frac{k}{2r} + O(m/r^2). \quad (2.22)$$

$\tilde{\Phi}_{22}$ works the same way, establishing the relation between the charge and the size of the Nahm matrices. We will use similar techniques below to calculate approximate monopole fields.

The construction is remarkably easy to implement in the case of a single $SU(2)$ monopole, where it even predates the Nahm equation [20]. For $k = 1$ the Nahm matrices reduce to numerical functions of s . The Nahm equations imply that these must be constants, which turn out to give the position of the monopole. By translational invariance, this can be taken to be the origin. Thus

$$v_a(s; \mathbf{r}) = N(\mathbf{r}) e^{\mathbf{r} \cdot \boldsymbol{\sigma} s} v_a^0(\mathbf{r}) \quad (2.23)$$

where the v_a^0 are orthonormal and the normalization factor

$$N = \sqrt{2r} e^{-mr/2} [1 - e^{-2mr}]^{-1/2} \quad (2.24)$$

is obtained by noting that

$$\int_{-m/2}^{m/2} e^{2\mathbf{r}\cdot\boldsymbol{\sigma}s} ds = \frac{\sinh mr}{r} \mathbf{I}_2 \quad (2.25)$$

Because

$$\int_{-m/2}^{m/2} s e^{2\mathbf{r}\cdot\boldsymbol{\sigma}s} ds = \frac{1}{2r^3} (mr \cosh mr - \sinh mr) \mathbf{r} \cdot \boldsymbol{\sigma} \quad (2.26)$$

the Higgs field is

$$\Phi_{ab}(\mathbf{r}) = \frac{1}{2} \left(m \coth mr - \frac{1}{r} \right) v_a^{0\dagger} \hat{\mathbf{r}} \cdot \boldsymbol{\sigma} v_b^0. \quad (2.27)$$

The usual ‘‘hedgehog gauge’’ form of the one-monopole Higgs field is obtained by taking $v_1^0 = (1, 0)^t$ and $v_2^0 = (0, 1)^t$. Another possibility is

$$v_1^0 = \psi(\mathbf{r}) \quad v_2^0 = \bar{\psi}(\mathbf{r}) \quad (2.28)$$

where the two-component spinors

$$\psi(\mathbf{r}) = \sqrt{\frac{r-z}{2r}} \begin{pmatrix} \frac{x-iy}{r-z} \\ 1 \end{pmatrix} \quad \bar{\psi}(\mathbf{r}) = \sqrt{\frac{r-z}{2r}} \begin{pmatrix} 1 \\ -\frac{x+iy}{r-z} \end{pmatrix}, \quad (2.29)$$

which are eigenvectors of $\hat{\mathbf{r}} \cdot \boldsymbol{\sigma}$ with eigenvalues ± 1 , satisfy $\psi^\dagger \psi = \bar{\psi}^\dagger \bar{\psi} = 1$, $\psi^\dagger \bar{\psi} = 0$. With this choice, the Higgs field is everywhere proportional to σ_3 . The singularity in $\psi(\mathbf{r})$ along the positive z -axis is the Dirac string that appears whenever a monopole solution is written with a uniform Higgs field direction.

B. The Nahm construction for $\text{SU}(N)$

For $\text{SU}(2)$ monopoles, the boundary values of s are given by the two eigenvalues $\pm m/2$ of the asymptotic Higgs field Φ_0 . In the case of $\text{SU}(N)$ monopoles, the asymptotic Higgs field has more than two eigenvalues and the Nahm data are matrix functions over a subdivided interval defined by the eigenvalues. In order to describe this, it is convenient to choose a particular basis for the Cartan generators. We choose diagonal generators H_i so that

$$\Phi_0 = \mathbf{h} \cdot \mathbf{H} = \text{diag}(s_N, s_{N-1}, \dots, s_1) \quad (2.30)$$

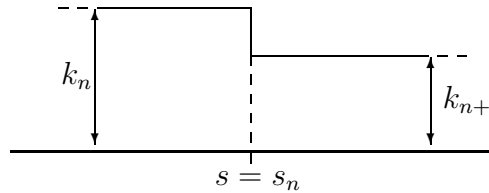
where $s_1 \leq s_2 \leq \dots \leq s_N$. In the case of maximal symmetry breaking, none of these eigenvalues are equal and so all the inequalities are strict. The magnetic charge is

$$Q_M = 4\pi \operatorname{diag}(k_{N-1}, k_{N-2} - k_{N-1}, \dots, k_1 - k_2, -k_1). \quad (2.31)$$

With this basis of Cartan generators, the n th fundamental monopole, with $k_m = \delta_{nm}$, is obtained by embedding an appropriately rescaled $SU(2)$ monopole solution in the 2×2 block at the intersection of the $(N - n)$ th and $(N + 1 - n)$ th rows and columns. This fundamental monopole then has mass $2\pi(s_{n+1} - s_n)$.

In the Nahm construction, the corresponding Nahm data are defined on an interval divided into $N - 1$ subintervals: (s_1, s_2) , (s_2, s_3) , and so on to (s_{N-1}, s_N) . Each of these subintervals can be thought of as corresponding to a different fundamental monopole. The size of the Nahm matrices over that interval is given by the number of monopoles of that type. Thus, the data reciprocal to a $(k_1, k_2, \dots, k_{N-1})$ monopole solution are $k_1 \times k_1$ matrices for $s \in (s_1, s_2)$, $k_2 \times k_2$ matrices for $s \in (s_2, s_3)$ and so on to $k_{N-1} \times k_{N-1}$ matrices for $s \in (s_{N-1}, s_N)$. The length of the subinterval determines the mass of the fundamental monopole. When describing Nahm data, it is sometimes useful to use a skyline diagram: a step function over the interval whose height in a subinterval is given by the size of the Nahm matrices in that subinterval.

There are boundary conditions relating the triplets (T_1, T_2, T_3) on either side of one of the subdivision points s_n . (There are no boundary conditions on T_0 .) If $k_n \neq k_{n+1}$ these boundary conditions are quite simple. For the skyline diagram



$$(2.32)$$

the Nahm triplet, (T_1, T_2, T_3) , is a triplet of $k_n \times k_n$ matrices over the left interval and of $k_{n+1} \times k_{n+1}$ matrices over the right interval. As $t = s - s_n$ approaches $0-$, it is required that

$$T_i(t) = \begin{pmatrix} R_i/t + O(1) & O(t^{(m-1)/2}) \\ O(t^{(m-1)/2}) & T'_i + O(t) \end{pmatrix} \quad (2.33)$$

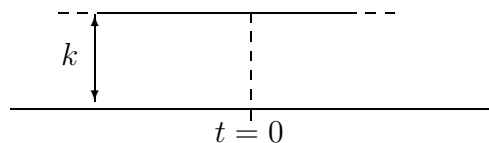
where $m = k_n - k_{n+1}$ and the $k_{n+1} \times k_{n+1}$ matrix T'_i is the nonsingular limit of the right interval Nahm data at $t = 0+$. The $m \times m$ residue matrices R_i in (2.33) must form an irreducible m -dimensional representation of $SU(2)$. Since the one-dimensional representation is trivial, there is no singularity when $m = 1$.

Thus, when the data are a different size on each side of a junction point, the smaller matrices match up continuously with sub-matrices of the larger matrices. The vector $v(t; \mathbf{r})$ in the construction equation is split in the same way, with k_n components carrying through the boundary:

$$v(t) = \begin{pmatrix} O(t^{(m-1)/2}) \\ v' \end{pmatrix} \quad (2.34)$$

where v' is the nonsingular limit from the right interval.

When $k_1 = k_2$ the situation is different. For the situation described by the skyline diagram



$$\quad (2.35)$$

the Nahm matrices may be discontinuous across $t = 0$. In fact, there are additional data, called jumping data, associated with the $t = 0$ junction. Let

$$\delta T_i = T_i(0-) - T_i(0+) \quad (2.36)$$

be the discontinuity in the Nahm matrices. The jumping data are a k -vector of 2-component spinors $a_{r\alpha}$ satisfying the jump equation

$$(\delta T_i)_{rs} = a_{r\alpha}^* (\sigma_i)_{\alpha\beta} a_{s\beta}. \quad (2.37)$$

The r and s run from one to k and α and β are spinor indices running from one to two.

There are also additional construction data, $S \in \mathbf{C}$, associated with the junction. The construction vector $v(t; \mathbf{r})$ obeys

$$\delta v = v(0-) - v(0+) = Sa \quad (2.38)$$

where here a is considered a $2k$ -vector rather than a k -vector of 2-spinors. This reordering of a is done in the obvious way; v could also be considered a k -vector of 2-spinors with the Nahm matrices acting on the vector index and the Pauli matrices acting on the spinor index.

The extra construction data S enter the inner product and in the construction of the fields. Let us write $V = (v_1, v_2, \dots, v_{N-1}; S_{p_1}, S_{p_2}, \dots)$ for the construction data. Here v_n is a solution to the construction equation in the interval (s_n, s_{n+1}) , with v_n and v_{n+1} satisfying the appropriate boundary conditions at $s = s_n$. The S_p 's are the jumping data at any point s_p where $k_n = k_{n+1}$. The number of these zero jumps is certainly less than $N - 2$, but depends on the charge. In this case,

$$\langle V|V' \rangle = \sum_{n=1}^{N-1} \int_{s_n}^{s_{n+1}} v_n^\dagger v_n' ds + \sum_p S_p^* S_p' \quad (2.39)$$

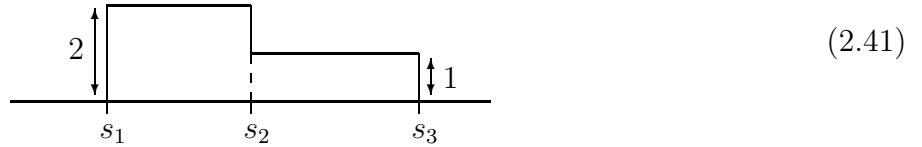
where p sums over the points where $k_n = k_{n+1}$. If $\{V_1, \dots, V_N\}$ is an orthonormalized basis for the construction data then

$$\begin{aligned} \Phi_{ab} &= \langle V_a | s | V_b \rangle = \sum_{n=1}^{N-1} \int_{s_n}^{s_{n+1}} (v_a)_n^\dagger s (v_b)_n ds + \sum_p (S_a)_p^* s_p (S_b)_p \\ (A_i)_{ab} &= -i \langle V_a | \partial_i | V_b \rangle = -i \left(\sum_{n=1}^{N-1} \int_{s_n}^{s_{n+1}} (v_a)_n^\dagger \partial_i (v_b)_n ds + \sum_p (S_a)_p^* \partial_i (S_b)_p \right). \end{aligned} \quad (2.40)$$

Of course, we have not shown that there is a N -dimensional family of solutions, or that the fields will have the right charge, or even that the fields satisfy the Bogomolny equation. In fact, all of these things are easily demonstrated using the same sort of argument as in the $SU(2)$ case described above [16,21].

If two s_i 's are coincident, there is a zero thickness subinterval in the Nahm interval. This means that there is a non-Abelian residual symmetry and some of the monopoles have zero mass. The boundary conditions for Nahm data in this situation can be described in terms of those explained above, by formally imagining the zero thickness subinterval as a limit of a subinterval of finite thickness. The Nahm data on this subinterval become irrelevant in the limit, but the height of the skyline on the vanishing subinterval affects the matching condition between the Nahm matrices over the subintervals on either side.

The skyline for a $(2,1)$ -monopole, for example, is given by



The Nahm data are 2×2 in the left interval and 1×1 in the right interval. The boundary conditions imply that the 2×2 data are nonsingular at the $s = s_2$ boundary with $T_i(s_2)_{2,2}$ equal to the 1×1 data. The data have a pole at $s = s_1$. If $s_2 = s_3$ the data are reciprocal to an $SU(3)$ $(2, [1])$ monopole solution. The skyline is



and the Nahm data are 2×2 matrices with a pole at $s = s_1$ but not at $s = s_2$. This is the Nahm data for the $(2, [1])$ monopole solution originally due to Dancer [11,12]. It will be discussed in greater detail in Sec. V.

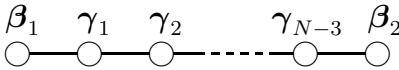


FIG. 1. $SU(N)$ Dynkin diagram with labeled roots.

III. PARAMETERS AND NAHM DATA

We are interested in the case

$$\Phi_0 = \text{diag}(s_R, s_0, s_0, \dots, s_0, s_L) \quad (3.1)$$

where the middle $N-2$ eigenvalues of Eq. (2.30) are equal, thus breaking the gauge symmetry to $U(1) \times SU(N-2) \times U(1)$. There are two types of massive monopoles and $N-3$ species of massless monopoles. Our labeling of the associated simple roots is indicated in the Dynkin diagram shown in Fig. 1.

With this symmetry breaking, the Nahm data consist of two triplets $T_i^L(s)$ and $T_i^R(s)$ that are defined on the intervals $(s_L, s_0]$ and $[s_0, s_R)$, respectively, as well as a set of complex column vectors a_p that form the jump data at s_0 .

In this section, we will identify the parameters that we expect to appear in our solutions and relate these to the Nahm data. Our goal is to study the $(2, [2], \dots, [2], 2)$ solutions. However, we will find it useful to first examine the $(1, [1], \dots, [1], 1)$ for $SU(N)$ and the $(2, [1])$ for $SU(3)$. Both of these cases have cloud parameters, and understanding these will be helpful in understanding the parameters of the $(2, [2], \dots, [2], 2)$ solution.

The dimension of the moduli space is equal to four times the total number of monopoles. However, there is one fewer moduli parameterizing the T_i and a_p Nahm data. This is because the modulus parameterizing the overall global $U(1)$ gauge rotation is associated only with T_0 and plays no role in the gauge that we have chosen for our Nahm construction. The remaining global gauge freedom will be present in our Nahm data, although for studying static nondyonic solutions we will not need to explicitly display the corresponding parameters and will usually work in a specific global gauge orientation.

A. $(1, [1], \dots, [1], 1)$ solutions for $SU(N)$

These solutions are composed of two massive and $N-3$ massless monopoles, and so form a $4(N-1)$ -dimensional moduli space. Six of the parameters can be chosen to specify the positions of the massive monopoles. The remaining parameters include a number of global gauge parameters as well as the parameters describing the gauge-invariant properties of the cloud.

Naively, one might expect the number of global gauge parameters to be $(N-2)^2+1$, since this is the dimension of the unbroken group. However, this cannot be correct in general; indeed, for large N this number far exceeds the total number of moduli available. In the case of $SU(4)$, it is easy to see that the full unbroken $U(1)\times SU(2)\times U(1)$ acts nontrivially on the solution, so the naive formula is correct here and there are, indeed, five global gauge parameters, leaving only a single cloud parameter.

For $N > 4$, the full set of solutions must include the subset obtained by embedding the $SU(4)$ solutions. These embedded solutions will be left invariant by a $U(N-4)$ subgroup of the unbroken gauge group, and thus will depend on

$$\dim[U(1) \times SU(N-2) \times U(1)/U(N-4)] = 4N - 11 \quad (3.2)$$

global gauge parameters. Together with the six position variables and the cloud parameter that is inherited from the $SU(4)$ solution, this accounts for all $4(N-1)$ parameters. Hence all the solutions lie in the global group orbit of the embedded solutions. This parameter-counting argument leaves open the possibility of a disconnected $4(N-1)$ -parameter family of solutions that are not $SU(4)$ embeddings, but the explicit Nahm construction of the fields rules this out [10].

With only one monopole of each type, the Nahm data are constants. Their values on the left and right interval, \mathbf{x}_L and \mathbf{x}_R respectively, specify the positions of the two massive monopoles. The jump data at s_0 are a set of $N-2$ two-component a_p that satisfy

$$\delta\mathbf{T} = \mathbf{x}_L - \mathbf{x}_R = \sum_{p=1}^{N-2} a_p^\dagger \boldsymbol{\sigma} a_p. \quad (3.3)$$

Thus, they comprise $4(N-2) - 3$ independent real numbers. Some of these are global gauge parameters associated with the $U(N-2)$ action that takes a_p to

$$a'_p = U_{pq} a_q. \quad (3.4)$$

Because there can only be two linearly independent two-component a_p , they can, at most, span a two-dimensional subspace of the $(N-2)$ -dimensional space on which the U_{pq} act. They are, therefore, invariant under a $U(N-4)$ subgroup, so the number of gauge parameters in the a_p is $\dim[U(N-2)/U(N-4)] = 4N - 12$. This leaves one nongauge parameter in the jump data; this parameter can be expressed as the single element of a 1×1 ‘‘matrix’’ T_4 defined by

$$T_4 \mathbf{I}_2 + \delta T_i \sigma_i = \sum_{p=1}^{N-2} a_p \otimes a_p^\dagger. \quad (3.5)$$

The eigenvalues of the matrix on the right-hand side are obviously positive. This translates into the condition $p \equiv T_4 \geq R$, where $R = |\mathbf{x}_L - \mathbf{x}_R|$. It turns out that p specifies the size of

the non-Abelian cloud. When it takes its minimum value, $p = R$, the right-side of Eq. (3.5) has rank one. There is then a $U(N - 2)$ transformation of the form of Eq. (3.4) that leaves only a single nonvanishing a_p , so the solution is, in fact, an embedding of a solution for $SU(3)$ broken to $U(1) \times U(1)$. Since there is no massless monopole in the $SU(3)$ theory, it is not surprising that this gives the minimal cloud.

It is instructive to compare these solutions with the $(1, 1, \dots, 1)$ solutions for maximally broken $SU(N)$. In the latter case, there are $N - 1$ intervals, in each of which the Nahm data is constant with value \mathbf{x}_n . At the boundary between two intervals, the jump data are determined, up to an irrelevant phase, by the analogue of Eq. (3.3). This implies, in particular, that at the n th boundary

$$a_n^\dagger a_n = |\mathbf{x}_n - \mathbf{x}_{n+1}|. \quad (3.6)$$

Examination of the spacetime fields for the case where the $|\mathbf{x}_n - \mathbf{x}_m|$ are all large shows that the \mathbf{x}_n are just the positions of the massive monopoles. In the limit where the middle $N - 3$ monopoles become massless and the corresponding intervals in the Nahm data shrink to zero width, the only remnant of these \mathbf{x}_n is their effect on the jump data. Thus, the effect of the $U(N - 2)$ action described above is to change the “positions” of the massless monopoles, subject only to the constraint that

$$p = \sum_{n=1}^{N-2} |\mathbf{x}_n - \mathbf{x}_{n+1}|. \quad (3.7)$$

In other words, p is a gauge invariant cloud parameter, but all the other position moduli are acted on by the group action.

B. $(2, [1])$ Dancer solutions for $SU(3)$

The solutions for one massless and two massive monopoles in $SU(3)$ broken to $SU(2) \times U(1)$ have been studied in detail [11,12,22,23]. Here we choose our conventions so that the eigenvalues of the Higgs vacuum expectation value are (s_0, s_0, s_L) , with $s_0 > s_L$. The Nahm data T_i are Hermitian 2×2 matrices on the interval $(s_L, s_0]$ that can be expanded as

$$T_i(s) = \frac{1}{2} \mathbf{C}_i(s) \cdot \boldsymbol{\tau} + R_i(s) \mathbf{I}_2. \quad (3.8)$$

Substituting this into the Nahm Eq. (2.1) show that the R_i are independent of s and the \mathbf{C}_i satisfy

$$\frac{d}{ds} \mathbf{C}_i = \frac{1}{2} \epsilon_{ijk} \mathbf{C}_j \times \mathbf{C}_k. \quad (3.9)$$

This means that the elements of the real symmetric matrix

$$M_{ij} = \mathbf{C}_i \cdot \mathbf{C}_j - \frac{1}{3} \delta_{ij} \mathbf{C}_k \cdot \mathbf{C}_k \quad (3.10)$$

are constants. If A is the s -independent real orthogonal matrix that diagonalizes M , the three vectors

$$\mathbf{B}_i(s) = A_{ji} \mathbf{C}_j(s) \quad (3.11)$$

are mutually orthogonal. Furthermore, substitution into Eq. (3.9) shows that the directions of these three vectors are independent of s , so that we can write

$$\mathbf{B}_i(s) = g_i(s) \hat{\mathbf{e}}_i \quad (3.12)$$

(with no implied sum over i) where the $\hat{\mathbf{e}}_i$ are three orthonormal vectors.

The Nahm equation then reduces to the Euler-Poinsot equations

$$\begin{aligned} \frac{dg_1}{ds} &= g_2 g_3 \\ \frac{dg_2}{ds} &= g_3 g_1 \\ \frac{dg_3}{ds} &= g_1 g_2. \end{aligned} \quad (3.13)$$

These imply that the three quantities $\Delta_{ij} = g_i^2 - g_j^2$ are constant, allowing us to order the \mathbf{B}_i so that $|g_1(s)| \leq |g_2(s)| \leq |g_3(s)|$. Fixing one constant of integration by the requirement that the T_i have a pole at s_L then gives

$$g_i(s) = f_i(s - s_L; k, D) \quad (3.14)$$

where the f_i are Euler top functions defined by

$$\begin{aligned} f_1(u; k, D) &= -D \frac{\text{cn}_k(Du)}{\text{sn}_k(Du)} \\ f_2(u; k, D) &= \mp D \frac{\text{dn}_k(Du)}{\text{sn}_k(Du)} \\ f_3(u; k, D) &= \mp \frac{D}{\text{sn}_k(Du)} \end{aligned} \quad (3.15)$$

with the elliptic parameter k lying in the range $0 \leq k \leq 1$. Note that there is a sign ambiguity in f_2 and f_3 ; to have a solution of the Euler-Poinsot equation, the same choice must be made for both functions. In our calculations we will have occasion to make use of both sign possibilities.

These top functions have poles at $u = 0$ and at $u = 2K(k)/D$, where $K(k)$ is the complete elliptic integral of the first kind. We have already arranged that the first pole is at the left boundary of the Nahm interval, $s = s_L$. The second pole must lie beyond the right boundary of the interval. This means that $2K/D > s_0 - s_L$ and we define a quantity a by

$$\frac{1}{a} = \frac{4K(k)}{D} - 2(s_0 - s_L). \quad (3.16)$$

Roughly, $2a$ measures the size of the top functions at s_0 . Since there is a half in the expression for T_i in Eq. (3.8), a determines the size of the matrix entries in the data. We will see that it is a cloud parameter.

The final result for the Nahm data is

$$T_i(s) = \frac{1}{2} \sum_{jk} A_{ij} f_j(s - s_L; k, D) E_{jk} \tau_k + R_i I_2 \quad (3.17)$$

where $E_{ij} \equiv (\hat{e}_i)_j$. The expression depends on eleven parameters. The nature of some of these is evident. The matrix E_{ij} depends on the three Euler angles that specify a global SU(2) gauge transformations. The three R_i specify the position of the center-of-mass. To understand the remaining five, it is easiest to first focus on the case where A is a unit matrix. From analysis of asymptotic cases and examination of numerical solutions for the spacetime fields [12,22,23] one finds that for large values of D there are two massive monopoles lying on the z -axis and separated by a distance D .

The effect of A is to rotate this configuration. Hence, two of the spatial Euler angles in A are directly related to the positions of the massive monopoles. The third Euler angle, corresponding to rotations about the axis joining the two monopoles, is a bit less obvious. Although one might expect a pair of monopoles to give an axially symmetric configuration, we know from the SU(2) example that this is not the case. The asymmetry falls exponentially with the monopole separation. At infinite separation, where the axial symmetry is recovered, rotations about this axis are equivalent to relative U(1) global gauge transformations of the two monopoles. For large, but finite, separation it is still most useful to view the corresponding Euler angle as being associated with a relative U(1) degree of freedom.

We choose the final parameter to be the quantity a that was defined in Eq. (3.16). Examination of solutions shows that a determines the size of the cloud. For large a , the cloud is approximately spherical with radius a . As a tends to infinity, the second pole of the Nahm data approaches the boundary of the interval, and the spacetime fields reduce to an embedding of the SU(2) two-monopole solution.

It is useful to consider the corresponding (2, 1) solution for SU(3) broken to U(1) \times U(1). Both species of monopoles are massive, with the Dancer solution corresponding to the limit where the second species becomes massless. For the (2, 1) case, the Nahm data in the left

hand interval are precisely the Dancer Nahm data discussed above. The Nahm data in the right hand interval, which specify the position of the monopole of the second type, are given by the vector $((T_1)_{22}, (T_2)_{22}, (T_3)_{22})$. One can show that when a is large it gives the approximate separation of the second type of monopole from the center of mass of the two monopoles of the first type. In the Dancer limit, this separation is the cloud parameter, but the direction of this separation has no effect on the Dancer solution. This example is discussed at length in [15].

C. $(2, [2], \dots, [2], 2)$ solutions for $SU(N)$

We now return to the case considered in Sec. III A, but with two monopoles, instead of one, of each type. A parameter-counting argument similar to that given in the previous case shows that for large N the generic solution is an embedding of an $SU(6)$ solution. We will therefore start by focusing on the case $N = 6$. The extension to larger N is straightforward, and we will discuss below the issues that arise when $N < 6$.

For the $SU(6)$ case, there are four massive and ten massless monopoles, and hence a 40-dimensional moduli space. There are 17 global gauge parameters, and we expect 12 more to specify the positions of the massive monopoles. This still leaves 11 parameters, enough to describe a much richer variety of solutions than were found in the previous cases.

By examining the Nahm data, we can clarify the interpretation of these last 11 parameters. On the left and right intervals the solutions of the Nahm equations are just those found for the Dancer solution, but with the arguments of the elliptic functions arranged so that the left and right Nahm data have their poles at s_L and s_R , respectively. Thus,

$$\begin{aligned} T_i^L(s) &= \frac{1}{2} \sum_{ij} A_{ij}^L f_j^L(s - s_L; k_L, D_L) \tau_j^L + R_i^L I_2 \\ T_i^R(s) &= \frac{1}{2} \sum_{ij} A_{ij}^R f_j^R(s - s_R + 2K/D_R; k_R, D_R) \tau_j^R + R_i^R I_2. \end{aligned} \quad (3.18)$$

where f_j^L (f_j^R) are the top functions given in Eq. 3.15 with the upper (lower) choice of sign; these choices of signs will prove convenient in subsequent calculations. Here we have defined two rotated triplets of Pauli matrices

$$\begin{aligned} \tau_i^L &= E_{ij}^L \tau_j \\ \tau_i^R &= E_{ij}^R \tau_j \end{aligned} \quad (3.19)$$

where the matrices E_{ij}^L and E_{ij}^R , each depending on three Euler angles, encode the effect of two independent $SU(2)$ transformations on the standard set of Pauli matrices.

The $T_i^L(s)$ and the $T_i^R(s)$ each contain 11 parameters. Six of these specify massive monopole positions: \mathbf{R} , D , and two of the Euler angles in the rotation matrix A . As

discussed above, the third Euler angle in A is related to relative U(1) rotations of the corresponding massive monopoles. In the Dancer $(2, [1])$ solution, a cloud parameter a was defined which depended on the distance between the end of the interval and the pole. In the SU(6) context, there are two such parameters, a_L and a_R . These will be called Dancer cloud parameters.

Finally, there are three SU(2) Euler angles in E . In the Dancer case, these were associated with global gauge transformations. Now that we have two sets of Dancer data, the relative SU(2) orientation of the $\boldsymbol{\tau}^L$ and $\boldsymbol{\tau}^R$ is a physical quantity and is a gauge-invariant property of the solutions. This is completely analogous to the relative U(1) in the SU(2) two-monopole solutions. On the other hand, a simultaneous SU(2) transformation of the $\boldsymbol{\tau}^L$ and $\boldsymbol{\tau}^R$ is still equivalent to a global gauge transformation of the solution.

The jump data consist of four a_p , each with four complex components. As in Subsec. II B, we view these as being two-component vectors whose components a_{pj} are themselves two-component spinors. There are 32 real parameters in the a_p . They obey a jump equation

$$(\delta T_i)_{rs} \equiv (T_i^L)_{rs} - (T_i^R)_{rs} = \sum_{p=1}^4 a_{pr}^\dagger \sigma_i a_{ps} \quad (3.20)$$

which gives 12 real constraints. Furthermore, there is an U(4) action, of the form of Eq. (3.4), that gives rise to 16 of the global gauge parameters. After subtracting these constraints and global gauge parameters, we are left with four parameters. These can be encoded in a 2×2 matrix

$$T_4 = pI_2 + \mathbf{q} \cdot \boldsymbol{\tau} \quad (3.21)$$

obeying

$$T_4 \otimes I_2 + \delta T_i \otimes \sigma_i = \sum_{p=1}^4 a_p \otimes a_p^\dagger. \quad (3.22)$$

In the spinor notation

$$T_4 = \sum_{p=1}^4 a_{pr}^\dagger a_{ps}. \quad (3.23)$$

We will see that p and \mathbf{q} encode information about clouds that are of a different type than the Dancer clouds; we will refer to these as SU(4)-cloud parameters. Eq. (3.22) forces $T_4 \otimes I_2 + \delta T_i \otimes \sigma_i$ to have positive eigenvalues. This constrains the cloud parameters. As we saw in Subsect. III A, this happens in the $(1, [1], \dots, [1], 1)$ case as well. Equation (3.22) is the same as Eq. (3.5), except that here we are dealing with matrices rather than numbers and, here, the constraints do not, in general, have a simple expression in terms of the other parameters.

There is some redundancy in the parameters that we have enumerated, in that the effects of a common SU(2) transformation of the $\boldsymbol{\tau}^L$ and $\boldsymbol{\tau}^R$ can be completely compensated by a U(4) action on the a_p , which in turn can rotate the direction of \mathbf{q} . Taking this factor into account, we have the following 23 nongauge degrees of freedom:

- a) 12 massive monopole position variables.
- b) Two relative U(1) parameters, one for the β_1 -monopoles and one for the β_2 -monopoles.
- c) Two Dancer cloud parameters, a_L and a_R .
- d) Two scalar SU(4) cloud parameters p and $q = |\mathbf{q}|$.
- e) Five parameters specifying the relative SU(2) orientations of the triplets $\boldsymbol{\tau}^L$ and $\boldsymbol{\tau}^R$ and the vector \mathbf{q} .

When the gauge group is smaller than SU(6), the number of parameters is reduced and additional constraints come into play. After the global gauge degrees of freedom are subtracted, the number of nongauge parameters remaining is 14 for SU(3), 19 for SU(4), and 22 for SU(5). This can be seen by counting the parameters arising from the jump data. For SU(N), there are $(N - 2)$ of the a_p , each with eight real components, that are subject to a U($N - 2$) gauge action. For $N = 3, 4$, and 5 , this gives seven, 12, and 15 nongauge variables in the jump data. However, there are 12 constraints imposed by Eq. (3.20). For SU(5), this means that T_4 has only three free variables. From Eq. (3.22), whose right hand side now has rank three, we see that these can be taken to be the components of \mathbf{q} , with p now fixed at its minimum value. For SU(4), counting arguments suggest that the constraints completely determine the jump data and that p and \mathbf{q} can be specified in terms of T_i^L and T_i^R . We will see that the actual situation is more subtle, and that not all values for T_i^L and T_i^R are possible; i.e., for some choices of Dancer data the constraints cannot be solved. For SU(3), there are more constraints than jump variables, so clearly T_i^L and T_i^R cannot be independently chosen Dancer-type Nahm data.

IV. $(k, [k], \dots, [k], k)$ MONOPOLES IN SU(N)

In the previous section, we saw that, for the $(1, [1], \dots, [1], 1)$ and the $(2, [2], \dots, [2], 2)$ cases, the solution of Nahm's equation can be reduced to an algebraic problem involving the jump data and the previously known Nahm data for the SU(2) unit monopole and the SU(3) $(2, [1])$ -solution. More generally, the Nahm data for the $(k, [k], \dots, [k], k)$ solution in SU(N) are clearly related to the Nahm data for the $(k, [k - 1], [k - 2], \dots, [1])$ solution for SU($k + 1$)

broken to $U(k)$. We will extend the term Dancer solutions to include these generalizations of the $SU(3)$ case.

We will show, in this section, that something similar happens when using the construction equation to calculate the spacetime fields from the data. Specifically, if the spacetime fields and the boundary values of the Nahm data and of the construction equation solutions are known for the Dancer problem, then the $SU(N)$ fields can be obtained by purely algebraic means. We will concentrate on the construction of the Higgs field, but the generalization to the gauge potential A_j is straightforward.

Throughout this section, we will assume that $N \geq 2k + 2$. The solutions for $N < 2k + 2$ can be obtained by constraining the Nahm data so that the $SU(2k + 2)$ solution is equivalent to an embedding of a solution from a smaller group.

The Nahm data on the left interval, $(s_L, s_0]$, are the $k \times k$ matrices $T_i^L(s)$ for the $SU(k + 1)$ Dancer problem, with their arguments chosen so that their poles are at s_L . These define a construction equation on this interval that has $k + 1$ linearly independent solutions $w_a^L(s; \mathbf{r})$, each of which is a $2k$ -component column vector. These satisfy

$$\int_{s_L}^{s_0} ds w_a^{L\dagger}(s; \mathbf{r}) w_b^L(s; \mathbf{r}) = \delta_{ab} \quad (4.1)$$

and give rise to an $SU(k + 1)$ Dancer solution with Higgs field

$$\varphi_{ab}^L(\mathbf{r}) = \int_{s_L}^{s_0} ds (s - s_0) w_a^{L\dagger}(s; \mathbf{r}) w_b^L(s; \mathbf{r}). \quad (4.2)$$

Similarly, the Nahm data $T_i^R(s)$ on the right interval lead to $k + 1$ solutions w_a^R that generate a Higgs field

$$\varphi_{ab}^R(\mathbf{r}) = \int_{s_0}^{s_R} ds (s - s_0) w_a^{R\dagger}(s; \mathbf{r}) w_b^R(s; \mathbf{r}). \quad (4.3)$$

In addition, there are the $2k$ -component a_p ($p = 1, \dots, N - 2$) that comprise the jump data at s_0 . By exploiting the $U(N - 2)$ action of Eq. (3.4), these can be chosen so that they satisfy a relation of the form

$$a_p^\dagger a_q = \lambda_p \delta_{pq} \quad (4.4)$$

for $p, q \leq 2k$, while $a_p = 0$ if $p > 2k$. Generalizing Eqs. (3.5) and (3.22), we now define

$$K = T_4 \otimes \mathbf{I}_2 + \delta T_i \otimes \sigma_i = \sum_p a_p \otimes a_p^\dagger. \quad (4.5)$$

As we saw in Sec. III, T_4 encodes the nongauge parameters in the a_p . As long as all $2k$ of the λ_p are nonzero, K is invertible, with

$$K^{-1} = \sum_{p=1}^{2k} \frac{1}{\lambda_p^2} a_p \otimes a_p^\dagger. \quad (4.6)$$

These data determine the form of the construction equation for the $SU(N)$ theory. We must find N linearly independent solutions V_a , each consisting of functions $v_a^L(s; \mathbf{r})$ and $v_a^R(s; \mathbf{r})$ defined on the intervals $(s_L, s_0]$ and $[s_0, s_R)$, respectively, and a set of $S_{ap}(\mathbf{r})$ defined at the jump. These must obey the orthonormality condition of Eq. (2.39). We proceed in two steps, first obtaining an intermediate set of solutions that are linearly independent but not orthonormal, and then orthonormalizing.

Thus, we define a set of $\tilde{V}_a(s; \mathbf{r})$ by requiring

$$\begin{aligned} \tilde{v}_a^L(s; \mathbf{r}) &= \begin{cases} w_{a-(k+1)}^L(s; \mathbf{r}), & k+2 \leq a \leq 2k+2 \\ 0, & \text{otherwise} \end{cases} \\ \tilde{v}_a^R(s; \mathbf{r}) &= \begin{cases} -w_a^R(s; \mathbf{r}), & 1 \leq a \leq k+1 \\ 0, & \text{otherwise.} \end{cases} \end{aligned} \quad (4.7)$$

(Note that both \tilde{v}_a^L and \tilde{v}_a^R vanish if $a > 2k+2$.) The discontinuity conditions on the \tilde{V}_a then take the form

$$V_a^0(\mathbf{r}) \equiv \tilde{v}_a^L(s_0; \mathbf{r}) - \tilde{v}_a^R(s_0; \mathbf{r}) = \sum_p \tilde{S}_{ap}(\mathbf{r}) a_p. \quad (4.8)$$

The orthonormality condition on the a_p , Eq. (4.4), determines the \tilde{S}_{ap} for $p \leq 2k$ to be

$$\tilde{S}_{ap} = \frac{1}{\lambda_p} a_p^\dagger V_a^0, \quad p \leq 2k. \quad (4.9)$$

The \tilde{S}_{ap} for $p > 2k$ are undetermined; we make the choice

$$\tilde{S}_{ap} = \delta_{(a-2),p}, \quad p > 2k. \quad (4.10)$$

These solutions are not properly orthonormalized. Instead,

$$\langle \tilde{V}_a | \tilde{V}_b \rangle = \begin{cases} B_{ab} & a, b \leq 2k+2 \\ \delta_{ab} & a, b > 2k+2 \\ 0 & \text{otherwise} \end{cases} \quad (4.11)$$

where B is a $(2k+2) \times (2k+2)$ matrix with

$$\begin{aligned} B_{ab} &= \delta_{ab} + \sum_{p=1}^{2k} \frac{1}{\lambda_p^2} (V_a^{0\dagger} a_p) (a_p^\dagger V_b^0) \\ &= \delta_{ab} + V_a^{0\dagger} K^{-1} V_b^0. \end{aligned} \quad (4.12)$$

B is clearly a Hermitian matrix with positive eigenvalues, so $B^{-1/2}$ exists. We can therefore define a new set of solutions by

$$V_a = \begin{cases} \tilde{V}_b (B^{-1/2})_{ba}, & a \leq 2k + 2 \\ \tilde{V}_a, & a > 2k + 2. \end{cases} \quad (4.13)$$

It is easily verified that these V_a are orthonormal. Following Eq. (2.40), they give rise to a Higgs field

$$\begin{aligned} \Phi_{ab} &= \langle V_a | s | V_b \rangle \\ &= \langle V_a | (s - s_0) | V_b \rangle + s_0 \delta_{ab}. \end{aligned} \quad (4.14)$$

In the second line, the first term gets contributions from the $v_a^L(s; \mathbf{r})$ and the $v_a^R(s; \mathbf{r})$, but not from the S_{ap} . As a result, it can be nonzero only if $1 \leq a, b \leq 2k + 2$. Hence if $N > 2k + 2$, the Higgs field is essentially an embedding of an $SU(2k + 2)$ field. Similarly, one can show that A_i can be written as an embedded solution. We lose little generality, but gain simplification in the notation, by henceforth assuming that $N = 2k + 2$. This allows us to write

$$\begin{aligned} \Phi_{ab} &= (B^{-1/2})_{ac} \langle \tilde{V}_c | (s - s_0) | \tilde{V}_d \rangle (B^{-1/2})_{da} + s_0 \delta_{ab} \\ &= (B^{-1/2})_{ac} \varphi_{cd} (B^{-1/2})_{da} + s_0 \delta_{ab} \end{aligned} \quad (4.15)$$

where φ is block diagonal:

$$\varphi = \begin{pmatrix} \varphi^R & 0 \\ 0 & \varphi^L \end{pmatrix}. \quad (4.16)$$

Because our main interest in this paper is in the massless monopole clouds, we can simplify our analysis by restricting our attention to the region of space lying outside the cores of the massive monopoles. Outside these cores, there is a clear distinction between the massless degrees of freedom associated with the unbroken gauge group and the fields that acquire masses through the symmetry breaking. When we apply the Nahm construction to our problem, this distinction appears as follows. As we will show explicitly for the cases $k = 1$ and $k = 2$, the solutions of the construction equation defined by the Dancer Nahm data can be chosen so that one of the $v_a(s; \mathbf{r})$ is concentrated near the side of the interval where the T_i have a pole and is exponentially small at the other side, while the remaining $v_a(s; \mathbf{r})$ are all concentrated on the side away from the pole.² The massive Higgs and gauge fields involve integrals containing products of the first v_a and one of the latter, and so

²This prescription for the $v_a(s; \mathbf{r})$ is a choice of gauge. It can be done locally without any problem, but extending it over all of space introduces Dirac string singularities.

fall exponentially with distance from the nearest massive monopole core. Ignoring these exponentially small terms, we can write the Dancer Higgs fields in the block diagonal forms

$$\begin{aligned}\varphi^R &= \begin{pmatrix} \phi^R & 0 \\ 0 & \hat{\varphi}^R \end{pmatrix} + \varphi_\infty^R \\ \varphi^L &= \begin{pmatrix} \hat{\varphi}^L & 0 \\ 0 & \phi^L \end{pmatrix} + \varphi_\infty^L.\end{aligned}\tag{4.17}$$

Here φ_∞^R and φ_∞^L are diagonal matrices corresponding to the Higgs expectation values of the Dancer solutions. Because ϕ^R and ϕ^L are purely U(1) fields, it is easy to see that they must be sums of poles of the form $\pm 1/r_n$ where r_n is the distance from the n th massive monopole and the upper and lower sign apply to ϕ^L and ϕ^R , respectively. The non-Abelian parts of the Dancer solutions are contained in the $k \times k$ matrices $\hat{\varphi}^R$ and $\hat{\varphi}^L$.

A similar decomposition occurs for B , which can be written in the block diagonal form

$$B = \begin{pmatrix} 1 & 0 & 0 \\ 0 & \hat{B} & 0 \\ 0 & 0 & 1 \end{pmatrix}.\tag{4.18}$$

Here \hat{B} is given by an expression of the same form as Eq. (4.12), but with the indices only running over the $2k$ values corresponding to the v_a that are nonvanishing near s_0 . Finally, Φ can be written as

$$\Phi = \begin{pmatrix} \phi^R & 0 & 0 \\ 0 & \hat{\Phi} & 0 \\ 0 & 0 & \phi^L \end{pmatrix} + \Phi_\infty\tag{4.19}$$

where the $2k \times 2k$ non-Abelian part of the Higgs field is

$$\hat{\Phi} = \hat{B}^{-1/2} \hat{\varphi} \hat{B}^{-1/2}\tag{4.20}$$

and $\hat{\varphi}$ is a block diagonal matrix

$$\hat{\varphi} = \begin{pmatrix} \hat{\varphi}^R & 0 \\ 0 & \hat{\varphi}^L \end{pmatrix}.\tag{4.21}$$

From Eq. (4.20) we can see quite clearly the role of the cloud parameters in the a_p . Note first that the scale of the V_a^0 is set by the distances to the massive monopoles and by the Dancer cloud parameters. If the a_p are all large compared to these, the eigenvalues of K^{-1} will be small, \hat{B} will be approximately a unit matrix, and the non-Abelian fields of the SU(N) solution will simply be those inherited from the two Dancer solutions. If, instead, the a_p are all small, the eigenvalues of K^{-1} will be large, \hat{B} will be large, and the factors of $\hat{B}^{-1/2}$ will suppress the non-Abelian part of the SU(N) fields.

These two cases correspond to being inside and outside a non-Abelian cloud of a type similar to those found in the previously known examples that were discussed in the introduction. There are two new features here, however. First, there are now k^2 cloud parameters contained in the a_p . Second, there are additional cloud parameters, of a somewhat different type, contained in the Dancer-type solutions. One of our goals in this work is to understand the interplay between these different types of clouds. In Sec. VI, we will examine these for the $k = 2$ case, after first having obtained some necessary results about the SU(3) Dancer solution. First, however, we will apply the formalism that we have just developed to the $k = 1$ case, verifying that we recover the results of Ref. [10] for the $(1, [1], 1)$ SU(4) case.

For $k = 1$, the ‘‘Dancer’’ solution is simply the unit SU(2) monopole solution. We take the two massive monopoles to lie along the z -axis, with the β_1 -monopole at $\mathbf{x}_R = (0, 0, -R/2)$ and the β_2 -monopole at $\mathbf{x}_L = (0, 0, R/2)$. From Eq. (3.5) we have $K = p + R\sigma_3$, and hence

$$K^{-1} = \frac{p - R\sigma_3}{p^2 - R^2}. \quad (4.22)$$

The solution of the construction equation for the unit monopole was given in Sec. II. Using Eqs. (2.23) and (2.24), we can take the solutions of the construction equations for the right and left Dancer problems to be

$$\begin{aligned} w_1^R(s; \mathbf{r}) &= \sqrt{2r_R} \left[1 - e^{-2r_R(s_R - s_0)} \right]^{-1/2} e^{-r_R(s_R - s)} \psi_R \\ w_2^R(s; \mathbf{r}) &= \sqrt{2r_R} \left[1 - e^{-2r_R(s_R - s_0)} \right]^{-1/2} e^{-r_R(s - s_0)} \bar{\psi}_R \\ w_1^L(s; \mathbf{r}) &= \sqrt{2r_L} \left[1 - e^{-2r_L(s_0 - s_L)} \right]^{-1/2} e^{-r_L(s_0 - s)} \psi_L \\ w_2^L(s; \mathbf{r}) &= \sqrt{2r_L} \left[1 - e^{-2r_L(s_0 - s_L)} \right]^{-1/2} e^{-r_L(s - s_L)} \bar{\psi}_L. \end{aligned} \quad (4.23)$$

Here $\mathbf{r}_R = \mathbf{r} - \mathbf{x}_R$ and $\mathbf{r}_L = \mathbf{r} - \mathbf{x}_L$, while $\psi_R = \psi(\mathbf{r}_R)$ and $\psi_L = \psi(\mathbf{r}_L)$ with $\psi(\mathbf{r})$ given by Eq. (2.29).

When $(s_R - s_0)r_R$ and $(s_0 - s_L)r_L$ are both large, $w_1^R(s; \mathbf{r})$ and $w_2^L(s; \mathbf{r})$ are concentrated near s_R and s_L , respectively, and are exponentially small at s_0 , while $w_2^R(s; \mathbf{r})$ and $w_1^L(s; \mathbf{r})$ peak at s_0 . Up to exponentially small corrections, the corresponding Higgs fields take the block diagonal form of Eq. (4.17), with $\phi^R = -1/2r_R$, $\phi^L = 1/2r_L$, and $\hat{\phi}^R$ and $\hat{\phi}^L$ combining to give

$$\hat{\phi} = \begin{pmatrix} 1/2r_R & 0 \\ 0 & -1/2r_L \end{pmatrix}. \quad (4.24)$$

To construct the matrix \hat{B} , we exclude the exponentially small U(1) components of V^0 , obtaining a reduced vector \hat{V}^0 . Using Eq. (4.23), we have (up to exponentially small corrections)

$$\begin{aligned}\hat{V}_1^0(\mathbf{r}) &= w_2^R(s; \mathbf{r}) = \sqrt{2r_R} \bar{\psi}_R \\ \hat{V}_2^0(\mathbf{r}) &= w_1^L(s; \mathbf{r}) = \sqrt{2r_L} \psi_L.\end{aligned}\tag{4.25}$$

Hence,

$$\begin{aligned}\hat{B} &= \mathbb{I}_2 + \hat{V}^{0\dagger} K^{-1} \hat{V}^0 \\ &= \mathbb{I}_2 + \frac{1}{p^2 - R^2} \begin{pmatrix} r_R \bar{\psi}_R^\dagger (p - R\sigma_3) \bar{\psi}_R & 2\sqrt{r_L r_R} \bar{\psi}_R^\dagger (p - R\sigma_3) \psi_L \\ 2\sqrt{r_L r_R} \psi_L^\dagger (p - R\sigma_3) \bar{\psi}_R & 2r_L \psi_L^\dagger (p - R\sigma_3) \psi_L \end{pmatrix}.\end{aligned}\tag{4.26}$$

Using the form of the spinors given in Eq. (2.29), together with the identities

$$\begin{aligned}z_L + z_R &= \frac{r_R^2 - r_L^2}{R} \\ z_L z_R &= \frac{1}{4R^2} [(r_R^2 - r_L^2)^2 - R^2],\end{aligned}\tag{4.27}$$

allows \hat{B} to be simplified to

$$\hat{B} = \frac{r_L + r_R + p}{p^2 - R^2} [p - R \hat{\mathbf{q}} \cdot \boldsymbol{\tau}]\tag{4.28}$$

where the unit vector $\hat{\mathbf{q}}$ has components

$$\hat{q}_i = \begin{cases} \frac{2r_i}{\sqrt{(r_L + r_R)^2 - R^2}} & i = 1, 2 \\ \frac{r_L - r_R}{R} & i = 3. \end{cases}\tag{4.29}$$

(For $i = 1$ and 2 we have used $x_L = x_R = x$ and $y_L = y_R = y$.)

Let U be the unitary matrix that rotates τ_3 to $\hat{\mathbf{q}} \cdot \boldsymbol{\tau}$, and define

$$L = \frac{p - R\tau_3}{r_L + r_R + p}.\tag{4.30}$$

Then $\hat{B} = UL^{-1}U^{-1}$ and

$$\hat{\Phi} = UL^{1/2} \left[\left(\frac{1}{4r_R} - \frac{1}{4r_L} \right) \mathbb{I}_2 - \left(\frac{1}{4r_R} + \frac{1}{4r_L} \right) \hat{\mathbf{q}} \cdot \boldsymbol{\tau} \right] L^{1/2} U^{-1}.\tag{4.31}$$

Taking into account that our cloud parameter p is equal to the quantity $2b + R$ of Ref. [10], we see that $\hat{\Phi}$ is the same, up to a gauge transformation by U , as the previously obtained expression.

V. (2,[1]) MONOPOLE SOLUTIONS AND THEIR FIELDS

In this section, we return to the (2, [1]) monopole solutions. The Nahm data for these monopoles were discussed in Sec. III. The Nahm construction of the monopole fields corresponding to these data has not proven to be tractable. However, as we describe in this section, it is possible to calculate useful approximate fields in certain situations. Along with the methods explained in the previous section, the (2, [1]) monopole construction allows us to construct (2, [2], ..., 2) monopole solutions in $SU(N)$. This will be considered in the next section.

Because we are primarily interested in the regions outside of the massive monopole cores, we can work in the infinite mass limit with data on the interval $(-\infty, s_0]$. In order for the Euler top functions introduced in Eq. (3.15) to be analytic on this semi-infinite interval, the elliptic parameter k must be unity, implying³

$$\begin{aligned} f_1^L &= f_2^L = -D \operatorname{cosech} D(s - s_0 - \epsilon) \\ f_3^L &= -D \operatorname{coth} D(s - s_0 - \epsilon) \end{aligned} \quad (5.1)$$

where $\epsilon = 1/2a$.

Further simplification occurs in two special cases. The first, that of minimal Dancer cloud, corresponds to $\epsilon \gg 1$. The other, that of large Dancer cloud, corresponds to $a/D \gg 1$.

A. Minimal Dancer cloud

If $\epsilon \rightarrow \infty$, the top functions become $f_1^L = f_2^L = 0$ and $f_3^L = D$ and the Nahm data of Eq. (3.17) reduce to

$$\begin{aligned} T_i(s) &= \frac{1}{2} D_i \tau'_3 + R_i I_2 \\ &= X_i^1 \left(\frac{\tau'_3 + I_2}{2} \right) + X_i^2 \left(\frac{\tau'_3 - I_2}{2} \right) \end{aligned} \quad (5.2)$$

where the $\tau'_i = E_{ij} \tau_j$ are a set of rotated Pauli matrices, $D_i = A_{i3} D$, and $\mathbf{X}^1 = \mathbf{R} + \mathbf{D}/2$ and $\mathbf{X}^2 = \mathbf{R} - \mathbf{D}/2$ are the positions of the two massive monopoles.

³This $k = 1$ limit is familiar as the hyperbolic monopole data discussed by Dancer in Ref. [24]. There is a subtle difference however, here we are interested in the infinite mass limit and so it is the location $s = s_L$ pole that is being sent to $s = -\infty$. In Ref. [24] the location of the second pole is sent to $s = \infty$. This difference affects the signs of the hyperbolic functions in the $k = 1$ limit. Since it is convenient to have all the signs identical in Eq. 5.1, these signs have been absorbed into the definition of f_i^L .

There is no pole in the Nahm data and the construction equation can be put into a block diagonal form with a separate 2×2 block corresponding to each of the two massive monopoles. Its solutions can be read off from the solutions to the one-monopole construction equation found in Sec. II. The two solutions that are nonzero at s_0 have boundary values

$$\begin{aligned} v_1^L(s_0) &= \sqrt{2r_1} \psi(\mathbf{r}_1) \otimes \chi_+ \\ v_2^L(s_0) &= \sqrt{2r_2} \psi(\mathbf{r}_2) \otimes \chi_- \end{aligned} \quad (5.3)$$

where r_1 and r_2 are the distances to the massive monopoles and χ_{\pm} are eigenvectors of τ'_3 with eigenvalues ± 1 . We have inserted a superscript L because the interval $(-\infty, s_0]$ corresponds to the left interval for the $SU(N)$ Nahm data. After a constant factor is extracted, the non-Abelian part of the Higgs field is

$$\hat{\phi}^L = \begin{pmatrix} -\frac{1}{2r_1} & 0 \\ 0 & -\frac{1}{2r_2} \end{pmatrix}. \quad (5.4)$$

This field corresponds to the massless monopole being coincident with one of the two massive monopoles.

Following a similar procedure on the right interval, $[s_0, \infty)$, leads to

$$\begin{aligned} v_1^R(s_0) &= \sqrt{2r_1} \bar{\psi}(\mathbf{r}_1) \chi_+ \\ v_2^R(s_0) &= \sqrt{2r_2} \bar{\psi}(\mathbf{r}_2) \chi_- \end{aligned} \quad (5.5)$$

and

$$\hat{\phi}^R = \begin{pmatrix} \frac{1}{2r_1} & 0 \\ 0 & \frac{1}{2r_2} \end{pmatrix}. \quad (5.6)$$

B. Small separation of the massive monopoles

We now consider the case where the separation of the two massive monopoles is small compared to the other scales of interest. In the limit $D \rightarrow 0$, the data are spherically symmetric, with three equal top functions

$$f_i^L = -\frac{1}{s - s_0 - \epsilon} \quad (5.7)$$

and Nahm matrices

$$T_i(s) = -\frac{1}{2} \frac{1}{s - s_0 - \epsilon} \tau'_i \quad (5.8)$$

where now $\tau'_i = A^{ij} E^{jk} \tau_k$. If we think of the massless monopole as being positioned at $((T_1)_{22}, (T_2)_{22}, (T_3)_{22})$, then it lies on a sphere of radius $a = 1/2\epsilon$ about the two massive monopoles and is rotated by both the spatial rotations and the global gauge transformations. For simplicity, we begin by exploiting these symmetries to position the massless monopole at $(0, 0, a)$ (or equivalently, to set $\tau' = \tau$), and calculate the fields along the positive z -axis.

Hence, we want to solve

$$\frac{d}{ds} v = (r_i I_2 - T_i) \otimes \sigma_i v \equiv (X - T)v. \quad (5.9)$$

In a basis where $I_2 \otimes \sigma_i$ is block diagonal with diagonal blocks both equal to σ_i ,

$$X - T = \begin{pmatrix} \frac{1}{2(s - s_0 - \epsilon)} + r & 0 & 0 & 0 \\ 0 & -\frac{1}{2(s - s_0 - \epsilon)} - r & \frac{1}{s - s_0 - \epsilon} & 0 \\ 0 & \frac{1}{s - s_0 - \epsilon} & -\frac{1}{2(s - s_0 - \epsilon)} + r & 0 \\ 0 & 0 & 0 & \frac{1}{2(s - s_0 - \epsilon)} - r \end{pmatrix}. \quad (5.10)$$

Two of the equations decouple, giving

$$v_1 = N_1 \sqrt{s_0 - s + \epsilon} e^{r(s - s_0 - \epsilon)} \begin{pmatrix} 1 \\ 0 \\ 0 \\ 0 \end{pmatrix} \quad (5.11)$$

and

$$v_4 = N_4 \sqrt{s_0 - s + \epsilon} e^{-r(s - s_0 - \epsilon)} \begin{pmatrix} 0 \\ 0 \\ 0 \\ 1 \end{pmatrix}. \quad (5.12)$$

Since v_1 is a decaying solution as $s \rightarrow -\infty$, it is an acceptable solution to the construction solution. Choosing N_1 so that $\int_{-\infty}^{s_0} v_1^t v_1 ds = 1$, we have

$$v_1(s_0) = \frac{\sqrt{2}r}{\sqrt{r+a}} \begin{pmatrix} 1 \\ 0 \\ 0 \\ 0 \end{pmatrix}. \quad (5.13)$$

The corresponding component of the Higgs field is

$$\begin{aligned} \phi_{11} &= \int_{-\infty}^{s_0} s v_1^\dagger v_1 ds \\ &= s_0 - \frac{1}{r} + \frac{1}{2(r+a)}. \end{aligned} \quad (5.14)$$

The other two equations are coupled. We substitute

$$v_2(s) = \begin{pmatrix} 0 \\ p(s) \\ q(s) \\ 0 \end{pmatrix} \quad (5.15)$$

and find

$$\begin{aligned} 2(s - s_0 - \epsilon)(\dot{p} + rp) + p - 2q &= 0 \\ 2(s - s_0 - \epsilon)(\dot{q} - rq) + q - 2p &= 0 \end{aligned} \quad (5.16)$$

with overdots denoting differentiation with respect to s . These give the second order equation

$$\ddot{p} + \frac{2}{s - s_0 - \epsilon} \dot{p} - r^2 p + \frac{r}{s - s_0 - \epsilon} p - \frac{3}{4(s - s_0 - \epsilon)^2} p = 0 \quad (5.17)$$

which is a Bessel equation. We are interested in the decaying solution

$$p = -N_2 \frac{1}{[r(s_0 - s + \epsilon)]^{3/2}} e^{r(s - s_0 - \epsilon)} \quad (5.18)$$

with corresponding q :

$$q = N_2 \left(\frac{2}{\sqrt{r(s_0 - s + \epsilon)}} + \frac{1}{[r(s_0 - s + \epsilon)]^{3/2}} \right) e^{r(s - s_0 - \epsilon)}. \quad (5.19)$$

The normalization constant is fixed by requiring

$$1 = \int_{-\infty}^{s_0} (p^2 + q^2) ds = N_2(2I_3 + 4I_2 + 4I_1) \quad (5.20)$$

where

$$I_n = \int_{-\infty}^{s_0} \frac{1}{[r(s_0 - s + \epsilon)]^n} e^{2r(s - s_0 - \epsilon)} ds. \quad (5.21)$$

Integrating by parts shows that

$$I_{n+1} = \frac{1}{n} \left(\frac{1}{r^{n+1} \epsilon^n} e^{-2r\epsilon} - 2I_n \right) \quad (5.22)$$

for $n > 0$. I_0 can be integrated exactly and all the I_1 terms cancel, leading to

$$v_2(s_0) = \frac{\sqrt{2}r}{\sqrt{r+a}} \begin{pmatrix} 0 \\ 0 \\ 1 \\ 0 \end{pmatrix} + \frac{\sqrt{2}a}{\sqrt{r+a}} \begin{pmatrix} 0 \\ -1 \\ 1 \\ 0 \end{pmatrix}. \quad (5.23)$$

The corresponding component of the Higgs field is

$$\phi_{22} = \int_{-\infty}^{s_0} (p^2 + q^2) s ds = s_0 - \frac{1}{2(a+r)}. \quad (5.24)$$

Equations (5.14) and (5.24) give the diagonal elements of the Higgs field. The off-diagonal elements clearly vanish, since $v_1(s)$ and $v_2(s)$ are pointwise orthogonal. Hence, we have found that the non-Abelian part of the Higgs field is

$$\hat{\phi}^L = \begin{pmatrix} s_0 - \frac{1}{r} + \frac{1}{2(a+r)} & 0 \\ 0 & s_0 - \frac{1}{2(a+r)} \end{pmatrix} \quad (5.25)$$

when r and a are both much bigger than both the monopole core size and the monopole separation. This expression was previously derived in [23] using symmetry arguments. It exhibits the role played by the cloud. Inside the cloud, $r \ll a$ and

$$\hat{\phi}^L \approx \begin{pmatrix} s_0 + \epsilon - \frac{1}{r} & 0 \\ 0 & s_0 - \epsilon \end{pmatrix} \quad (5.26)$$

which is the field of the two massive monopoles. The only effect of the massless monopole is to modify the monopole mass. However, for $r \gg a$

$$\hat{\phi}^L \approx \begin{pmatrix} s_0 - \frac{1}{2r} & 0 \\ 0 & s_0 - \frac{1}{2r} \end{pmatrix}. \quad (5.27)$$

Thus, at large distance, there is a $\text{diag}(1/2r, -1/2r)$ contribution to the field from the massless monopole. In other words, the massless monopole charge screens the massive monopole charges at a distance scale of roughly a .

Up to now we have restricted ourselves to the case where \mathbf{r} is along the positive z -axis and the SU(2) orientation of the Dancer cloud is such that $\boldsymbol{\tau}' = \boldsymbol{\tau}$. The more general case can be obtained by applying appropriate symmetry transformations to our solution. Suppose that $\boldsymbol{\tau}' = U\boldsymbol{\tau}U^{-1}$, where

$$U = \begin{pmatrix} f & g \\ -g^* & f^* \end{pmatrix}. \quad (5.28)$$

For an arbitrary position, not necessarily on the z -axis, Eqs. (5.13) and (5.23) are then replaced by

$$\begin{aligned} v_1(s_0) &= \frac{\sqrt{2}r}{\sqrt{r+a}} \begin{pmatrix} \lambda_+ \psi(\mathbf{r}) \\ \lambda_- \psi(\mathbf{r}) \end{pmatrix} \\ v_2(s_0) &= \frac{\sqrt{2}r}{\sqrt{r+a}} \begin{pmatrix} -\lambda_-^* \psi(\mathbf{r}) \\ \lambda_+^* \psi(\mathbf{r}) \end{pmatrix} + \frac{\sqrt{2}a}{\sqrt{r+a}} \begin{pmatrix} g \\ -f \\ f^* \\ g^* \end{pmatrix} \end{aligned} \quad (5.29)$$

where the two-component vector $\psi(\mathbf{r})$ is defined by Eq. (2.29) and

$$\begin{aligned} \lambda_+ &= \sqrt{\frac{r-z}{2r}} \left[\frac{x-iy}{r-z} f + g \right] \\ \lambda_- &= \sqrt{\frac{r-z}{2r}} \left[f^* - \frac{x-iy}{r-z} g^* \right]. \end{aligned} \quad (5.30)$$

Equation (5.25) for the Higgs field remains unchanged.

Well outside the cloud, where $r \gg a$, the second term in $v_2^L(s_0)$ is suppressed by a factor of a/r . If this term is ignored, then a linear combination of the $v_j^L(s)$ gives an alternative basis, $v_j'^L(s)$, for which the boundary values

$$\begin{aligned} v_1'^L(s_0) &\approx \sqrt{2r} \begin{pmatrix} \psi(\mathbf{r}) \\ 0 \end{pmatrix} \\ v_2'^L(s_0) &\approx \sqrt{2r} \begin{pmatrix} 0 \\ \psi(\mathbf{r}) \end{pmatrix} \end{aligned} \quad (5.31)$$

are independent of the SU(2) rotation to leading order in a/r . The leading approximation to the Higgs field, Eq. (5.27), is unaffected by this change of basis and so is independent of the SU(2) orientation parameters in U .

Proceeding in the same manner on the interval $[s_0, \infty)$ leads to

$$v_1(s_0) = \frac{\sqrt{2}r}{\sqrt{r+a}} \begin{pmatrix} \mu_+ \bar{\psi}(\mathbf{r}) \\ \mu_- \bar{\psi}(\mathbf{r}) \end{pmatrix}$$

$$v_2(s_0) = \frac{\sqrt{2}r}{\sqrt{r+a}} \begin{pmatrix} -\mu_-^* \bar{\psi}(\mathbf{r}) \\ \mu_+^* \bar{\psi}(\mathbf{r}) \end{pmatrix} + \frac{\sqrt{2}a}{\sqrt{r+a}} \begin{pmatrix} g \\ -f \\ f^* \\ g^* \end{pmatrix} \quad (5.32)$$

with

$$\begin{aligned} \mu_+ &= \sqrt{\frac{r-z}{2r}} \left[f + \frac{x+iy}{r-z} g \right] \\ \mu_- &= -\sqrt{\frac{r-z}{2r}} \left[\frac{x+iy}{r-z} f^* + g^* \right]. \end{aligned} \quad (5.33)$$

The corresponding Higgs field has a non-Abelian component

$$\hat{\phi}^R = \begin{pmatrix} s_0 + \frac{1}{r} - \frac{1}{2(a+r)} & 0 \\ 0 & s_0 + \frac{1}{2(a+r)} \end{pmatrix}. \quad (5.34)$$

VI. EXPLICIT $(2, [2], [2], [2], 2)$ SOLUTIONS IN $SU(6)$

In this section, we will use the results of Sec. V on $SU(3)$ Dancer solutions, together with the general formalism developed in Sec. IV, to obtain $(2, [2], [2], [2], 2)$ solutions for $SU(6)$ broken to $U(1) \times SU(4) \times U(1)$. As previously, we will concentrate on the region outside the massive monopole cores. Hence, our primary interest will be in the non-Abelian part $\hat{\Phi}$ of the Higgs field. From Eq. (4.20), this is given by

$$\hat{\Phi} = \hat{B}^{-1/2} \hat{\varphi} \hat{B}^{-1/2} = \hat{B}^{-1/2} \begin{pmatrix} \hat{\varphi}^R & 0 \\ 0 & \hat{\varphi}^L \end{pmatrix} \hat{B}^{-1/2} \quad (6.1)$$

where the 2×2 matrices $\hat{\varphi}^L$ and $\hat{\varphi}^R$ are obtained from the Dancer solutions corresponding to the Nahm data on the left and right intervals (s_1, s_0) and $[s_0, s_2)$. The 4×4 matrix \hat{B} is

$$\hat{B} = \mathbf{I}_4 + \hat{V}^{0\dagger}(s_0) K^{-1} \hat{V}^0(s_0). \quad (6.2)$$

Here $\hat{V}^0(s_0)$ is obtained from the solutions of construction equations for the right and left Dancer solutions, while

$$K = [p\mathbf{I}_4 + \mathbf{q} \cdot \boldsymbol{\tau}] \otimes \mathbf{I}_2 + [T_i^L(s_0) - T_i^R(s_0)] \otimes \sigma_i. \quad (6.3)$$

For the remainder of this section we will omit the argument of \hat{V}^0 ; it should always be understood to be s_0 . Note that \hat{V}^0 depends on \mathbf{r} , while K does not.

In principle, as long as the left and right Dancer solutions are of one of the two types studied in Sec. V, we can obtain expressions for $\hat{\Phi}$ that are exact, up to exponentially small corrections, outside the massive cores. However, our primary goal is to understand the role played by the cloud parameters. In particular, we want to see how the clouds affect the non-Abelian magnetic fields. This can be summarized by a position-dependent magnetic charge Q_{NA} . For a spherically symmetric configuration, this can be immediately read off from the non-Abelian part of the Higgs field, with

$$\hat{\Phi} = -\frac{Q_{NA}}{2r} + O\left(\frac{1}{r^2}\right). \quad (6.4)$$

For less symmetric configurations, where the magnetic field has contributions from Coulomb fields centered at several different points \mathbf{x}_j , Q_{NA} is obtained by adding the coefficients of the $1/|\mathbf{r} - \mathbf{x}_j|$ terms in the Higgs field. With this goal in mind, we focus on several limiting cases in which the existence of small parameters makes it particularly easy to pick out the $1/r$ terms in the Higgs field.

A. Two minimal Dancer clouds

We first consider the case where both the left and right data correspond to Dancer clouds of minimal size. The massive monopoles are located at

$$\begin{aligned} \mathbf{x}_1 &= \mathbf{R}^R + \mathbf{D}^R \\ \mathbf{x}_2 &= \mathbf{R}^R - \mathbf{D}^R \\ \mathbf{x}_3 &= \mathbf{R}^L + \mathbf{D}^L \\ \mathbf{x}_4 &= \mathbf{R}^L - \mathbf{D}^L. \end{aligned} \quad (6.5)$$

We fix the SU(2) orientation of the SU(4) cloud so that $\mathbf{q} = (0, 0, q)$, but for the moment leave those of the two Dancer clouds arbitrary. This leads to

$$K = (p\mathbf{I}_2 + q\tau_3) \otimes \mathbf{I}_2 + (R_i + D_i^L \tau_3^L - D_i^R \tau_3^R) \otimes \sigma_i \quad (6.6)$$

where $\mathbf{R} = \mathbf{R}^L - \mathbf{R}^R$.

The solutions of the construction equation yield the boundary values

$$\hat{V}_j^0 = \sqrt{2r_j} s_j \otimes \chi_j. \quad (6.7)$$

Here, the quantities s_j and χ_j are defined by

$$\begin{aligned} \hat{V}_1^0(s_0) &= \sqrt{2r_1} \bar{\psi}(\mathbf{r}_1) \otimes \chi_+^R \\ \hat{V}_2^0(s_0) &= \sqrt{2r_2} \bar{\psi}(\mathbf{r}_2) \otimes \chi_-^R \end{aligned}$$

$$\begin{aligned}\hat{V}_3^0(s_0) &= \sqrt{2r_3} \psi(\mathbf{r}_3) \otimes \chi_+^L \\ \hat{V}_4^0(s_0) &= \sqrt{2r_4} \psi(\mathbf{r}_4) \otimes \chi_-^L\end{aligned}\tag{6.8}$$

where $\psi(\mathbf{r})$ is given by Eq. (2.29) and χ_\pm^L (χ_\pm^R) are eigenvectors of τ_3^L (τ_3^R) with eigenvalues ± 1 . These solutions also lead to

$$\hat{\varphi} = \frac{1}{2r} \text{diag}(1, 1, -1, -1).\tag{6.9}$$

We will analyze in detail three special cases:

- 1) SU(2) orientations of both Dancer clouds and the SU(4) cloud all aligned.
- 2) $\mathbf{x}_1 = \mathbf{x}_3$ and $\mathbf{x}_2 = \mathbf{x}_4$, with the Dancer clouds having identical SU(2) orientations.
- 3) Large SU(4) clouds: $p \pm q \gg |\mathbf{x}_i - \mathbf{x}_j|$ for all i, j .

1. All cloud SU(2)'s aligned

If the SU(2) orientations of the Dancer and SU(4) clouds are all identical, so that $\tau_3^R = \tau_3^L = \tau_3$, then

$$K = \left(\frac{\mathbf{I}_2 + \tau_3}{2}\right) \otimes [(p+q)\mathbf{I}_2 + (\mathbf{x}_3 - \mathbf{x}_1) \cdot \boldsymbol{\sigma}] + \left(\frac{\mathbf{I}_2 - \tau_3}{2}\right) \otimes [(p-q)\mathbf{I}_2 + (\mathbf{x}_4 - \mathbf{x}_2) \cdot \boldsymbol{\sigma}].\tag{6.10}$$

Because the \hat{V}_j^0 are all eigenvectors of τ^3 , the problem reduces to two independent problems, each equivalent to the SU(4) (1, [1], 1) problem discussed in Sec. IV. One yields an ellipsoidal SU(4) cloud with cloud parameter $p+q$ that encloses monopoles 1 and 3, while the other gives a cloud with parameter $p-q$ enclosing monopoles 2 and 4. Because the non-Abelian fields of the two clouds lie in mutually commuting SU(2) subgroups of the unbroken SU(4), the only interactions between the clouds are those from the short range interactions involving the massive monopole cores. Hence, the two clouds can be disjoint, one enclosed within the other, or, as shown in Fig. 2, overlapping.

2. Coincident massive monopoles

If there are pairs of coincident massive monopoles, with $\mathbf{x}_1 = \mathbf{x}_3$ and $\mathbf{x}_2 = \mathbf{x}_4$, then $D^L = D^R = D$ and $\mathbf{R} = 0$. If we also choose τ_3^L and τ_3^R to be identical, although not necessarily equal to τ^3 , then

$$K = (p\mathbf{I}_2 + q\tau_3) \otimes \mathbf{I}_2.\tag{6.11}$$

Substituting this, together with Eq. (6.8), into Eq. (6.2) yields

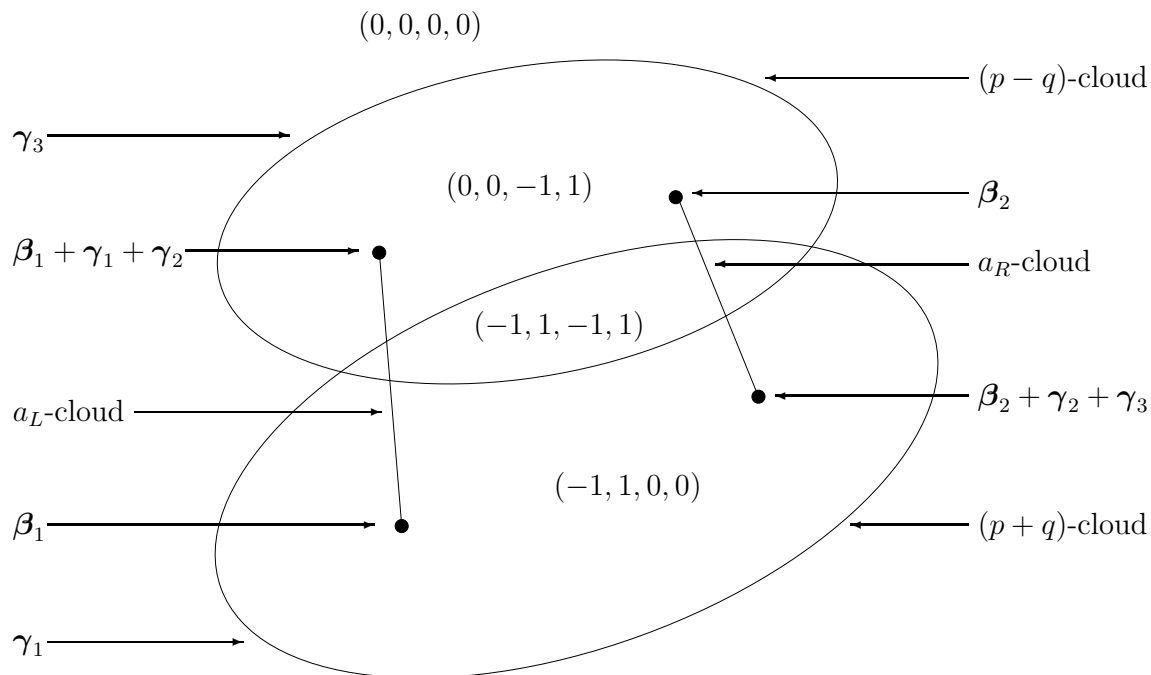


FIG. 2. A solution with two minimal Dancer clouds and all cloud $SU(2)$ orientations aligned. The clouds are labelled both by the relevant distance scale and by the associated massless monopole. As described in Sec. VII, the location of the massless monopoles at the end of the Dancer clouds is a gauge-dependent choice. The diagonal elements of Q_{NA} , which is assumed to be a diagonal matrix, are shown for each of the regions defined by the clouds.

$$\hat{B} = \mathbb{I}_2 + \frac{1}{p-q}M^- + \frac{1}{p+q}M^+ \quad (6.12)$$

where

$$M^\pm = 2\sqrt{r_i r_j} s_i^\dagger s_j (\chi_i^\dagger P_\pm \chi_j) \quad (6.13)$$

and $P_\pm = (\mathbb{I}_2 \pm \tau_3)/2$.

The s_j are fixed by the massive monopole positions and our definitions of $\psi(\mathbf{r})$ and $\bar{\psi}(\mathbf{r})$. We fix the χ_j by writing

$$\chi_+^L = \chi_+^R = \begin{pmatrix} c \\ d \end{pmatrix} \quad \chi_-^L = \chi_-^R = \begin{pmatrix} -d \\ c \end{pmatrix} \quad (6.14)$$

with c and d real.⁴ To normalize the spinors, we require $c^2 + d^2 = 1$. It then follows that

⁴For simplicity of notation, we have chosen the phases of the χ_j so that only real quantities appear in Eq. (6.14). One can verify that this has no effect on our final results.

$$c^2 - d^2 = \frac{1}{2} \text{Tr } \tau_3 \tau_3^L \equiv \cos \alpha. \quad (6.15)$$

Substitution of the explicit expressions for the s_j and the χ_j into Eq. (6.13) then gives

$$M^- = \begin{pmatrix} u^2 & uvf^* & 0 & uvg^* \\ uvf & v^2 & -uvf^* & 0 \\ 0 & -uvf & u^2 & uvf \\ uvf & 0 & uvf^* & v^2 \end{pmatrix} \quad (6.16)$$

where

$$\begin{aligned} u &= d\sqrt{r_1} \\ v &= c\sqrt{r_2} \\ f &= \psi(\mathbf{r}_1)^\dagger \psi(\mathbf{r}_2) \\ g &= \psi(\mathbf{r}_1)^\dagger \bar{\psi}(\mathbf{r}_2). \end{aligned} \quad (6.17)$$

(Note that $|f|^2 + |g|^2 = 1$.) The expression for M^+ can be obtained by making the substitutions $c \rightarrow d$ and $d \rightarrow -c$. The eigenvalues of M^- are doubly degenerate, with two being zero and two equal to $r_1 d^2 + r_2 c^2$; those of M^+ are zero and $r_1 c^2 + r_2 d^2$.

Let us now define

$$\begin{aligned} \lambda_- &= \frac{r_1 d^2 + r_2 c^2}{p - q} = \frac{(r_1 + r_2) + (r_2 - r_1) \cos \alpha}{2(p - q)} \\ \lambda_+ &= \frac{r_1 c^2 + r_2 d^2}{p + q} = \frac{(r_1 + r_2) - (r_2 - r_1) \cos \alpha}{2(p + q)}. \end{aligned} \quad (6.18)$$

We can then write

$$\begin{aligned} \hat{B} &= \mathbf{I}_4 + \lambda_- \left(\frac{2M^-}{\text{Tr } M^-} \right) + \lambda_+ \left(\frac{2M^+}{\text{Tr } M^+} \right) \\ &= \mathbf{I}_4 + \lambda_- \Pi^- + \lambda_+ \Pi^+ \end{aligned} \quad (6.19)$$

where Π^\pm are both projection operators. The spaces onto which they project are not in general mutually orthogonal; their overlap is measured by

$$\text{Tr } \Pi^+ \Pi^- = \frac{2(r_1 - r_2)^2 \sin^2 \alpha}{4r_1 r_2 + (r_1 - r_2)^2 \sin^2 \alpha} \leq 2. \quad (6.20)$$

This is small when r_1 and r_2 are both large compared to the monopole separation D , so far from the massive monopoles $\Pi^+ \approx \mathbf{I}_4 - \Pi^-$ and the eigenvalues of \hat{B} are approximately $1 + \lambda_-$ and $1 + \lambda_+$, both being doubly degenerate. For simplicity, let us assume that $p + q \gg D$. In

this case, λ_+ is non-negligible only in the large distance region where $\Pi^+ \approx \mathbf{I}_4 - \Pi^-$. Hence, \hat{B} can be approximated (everywhere) by

$$\hat{B} = (1 + \lambda_-)\Pi^- + (1 + \lambda_+)(\mathbf{I}_4 - \Pi^-). \quad (6.21)$$

The degree to which the non-Abelian charges are shielded, depends on the magnitudes of λ_- and λ_+ . If both are much less than unity, \hat{B} is approximately a unit matrix and there is no shielding by the SU(4) cloud. The field corresponds to an effective non-Abelian magnetic charge

$$Q_{\text{NA}} = \text{diag}(-1, -1, 1, 1). \quad (6.22)$$

If both are much greater than unity, there is complete shielding of the non-Abelian charge and $Q_{\text{NA}} = 0$. In the intermediate case, where $\lambda_- \gg 1$ but $\lambda_+ \ll 1$,

$$\hat{\Phi} \approx (\mathbf{I}_4 - \Pi^-)\hat{\varphi}(\mathbf{I}_4 - \Pi^-). \quad (6.23)$$

This corresponds to a charge that has only two nonzero eigenvalues, with the other two vanishing as a result of shielding by the cloud:

$$Q_{\text{NA}} = \text{diag}(-1, 0, 1, 0). \quad (6.24)$$

The boundaries between the regions corresponding to these three possibilities are roughly given by the surfaces $\lambda_+ = 1$ and $\lambda_- = 1$. Given our assumption that $p + q \gg D$, the former surface is approximately spherical, with radius $p + q$. The topology of the latter surface depends on the magnitude of $p - q$:

- 1) If $p - q > D(1 + |\cos \alpha|)/2$, the surface $\lambda_- = 1$ encloses all of the massive monopoles.
- 2) If $D(1 - |\cos \alpha|)/2 < p - q < D(1 + |\cos \alpha|)/2$, the surface $\lambda_- = 1$ encloses only one of \mathbf{x}_1 and \mathbf{x}_2 .
- 3) If $p - q < D(1 - |\cos \alpha|)/2$, then λ_- is always greater than unity. In this case, the unshielded charge of Eq. (6.22) never occurs.

Possibilities 1) and 2) are illustrated in Fig. 3.

3. Large SU(4) clouds

If $p + q$ and $p - q$ are both much larger than all of the $|\mathbf{x}_i - \mathbf{x}_j|$, then the first term on the right hand side of Eq. (6.6) dominates and K is well approximated by Eq. (6.11) and \hat{B} by Eq. (6.12). At short distances (all $r_j \ll p \pm q$), \hat{B} is approximately a unit matrix and one sees the unshielded charge of Eq. (6.22). At much larger distances, the r_j are all approximately equal. Equation (6.13) then gives

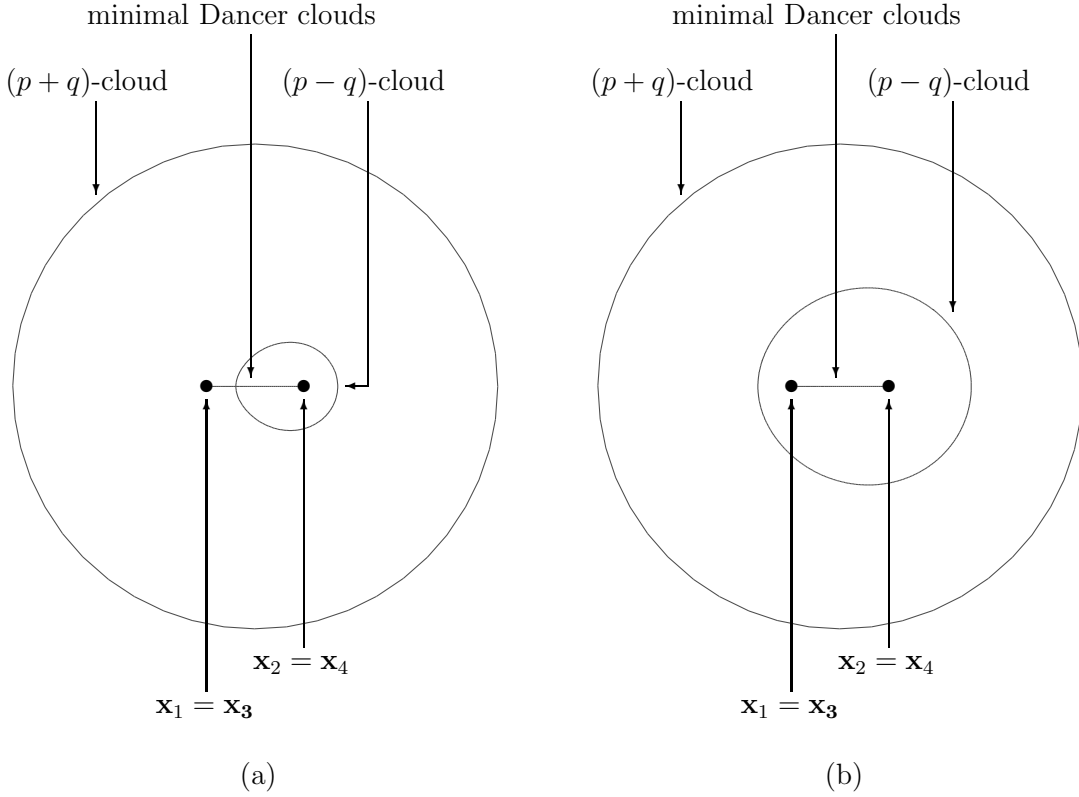


FIG. 3. Schematic illustration of a solution with minimal Dancer clouds and coincident massive monopoles, as discussed in Subsec. VI A 2. In both figures the $(p+q)$ -cloud is roughly defined by the curve $\lambda_+ = 1$ with $p+q = 5D$ and the $(p-q)$ -cloud by the curve $\lambda_- = 1$, where in (a) $p-q = 1.2D$ and in (b) $p+q = 2.2D$. In each case $\alpha = 4\pi/3$ and there are coincident β_1 - and β_2 -monopoles at $\mathbf{x}_1 = \mathbf{x}_3$ and at $\mathbf{x}_2 = \mathbf{x}_4$. The massless monopole locations are not shown, but calculating Q_{NA} in different regions indicates that there are γ_1 - and γ_3 -monopoles on the minimal Dancer clouds, a $(\gamma_2 + \gamma_3)$ -monopole on the $(p-q)$ -cloud and a $(\gamma_1 + \gamma_2)$ -monopole on the $(p+q)$ -cloud.

$$M^- \approx 2r \begin{pmatrix} c_R^2 & c_R d_R & 0 & 0 \\ c_R d_R & d_R^2 & 0 & 0 \\ 0 & 0 & c_L^2 & c_L d_L \\ 0 & 0 & c_L d_L & d_L^2 \end{pmatrix} \quad (6.25)$$

and

$$\frac{M^+}{2r} \approx \mathbb{I}_4 - \frac{M^-}{2r}. \quad (6.26)$$

(Here we have used the notation of Eq. (6.14), but have allowed for the possibility that the $SU(2)$ orientations of the left and right Dancer clouds might be different.) It follows that

$$\hat{B} \approx \frac{p-q+2r}{p-q} \frac{M^-}{2r} + \frac{p+q+2r}{p+q} \left(\mathbf{I}_4 - \frac{M^-}{2r} \right). \quad (6.27)$$

Because $M^-/2r$ is a projection operator, $\hat{B}^{-1/2}$ is easily calculated, and one obtains

$$\hat{\Phi} \approx \frac{1}{2r} U \begin{pmatrix} \frac{p-q}{p-q+2r} & 0 & 0 & 0 \\ 0 & \frac{p+q}{p+q+2r} & 0 & 0 \\ 0 & 0 & -\frac{p-q}{p-q+2r} & 0 \\ 0 & 0 & 0 & -\frac{p+q}{p+q+2r} \end{pmatrix} U^{-1} \quad (6.28)$$

where U is a unitary matrix that diagonalizes M^- . Hence, the non-Abelian magnetic charge is completely shielded for $r \gg p+q$, partially shielded, as in Eq. (6.24), for $p+q \gg r \gg p-q$, and unshielded for $r \ll p-q$.

B. Two large Dancer clouds

We now consider the case where both Dancer clouds are large. For convenience, we choose our spatial axes so that the “left cloud”, corresponding to the Nahm data $\mathbf{T}^L(s)$, is centered at $(0, 0, -R/2)$ and the “right cloud”, obtained from $\mathbf{T}^R(s)$ is centered at $(0, 0, R/2)$. We denote the distances from these two centers by r_L and r_R . The cloud parameters for the two clouds are a_L and a_R , while the $SU(2)$ orientations for the two clouds are encoded in the rotated triplets of Pauli matrices $\boldsymbol{\tau}^L$ and $\boldsymbol{\tau}^R$.

The matrix K is then

$$K = [p\mathbf{I}_2 + \mathbf{q} \cdot \boldsymbol{\tau}] \otimes \mathbf{I}_2 + R\mathbf{I}_2 \otimes \sigma_3 + a_R \tau_i^R \otimes \sigma_i + a_L \tau_i^L \otimes \sigma_i. \quad (6.29)$$

The $SU(4)$ cloud parameters p and \mathbf{q} must be such that the eigenvalues of K are all positive. We will write $q = |\mathbf{q}|$.

Three special cases are particularly easy to analyze:

- 1) Large $SU(4)$ cloud: $p \pm q \gg R, a_L, a_R$.
- 2) Widely separated Dancer clouds: $R \gg a_L, a_R$.
- 3) Two concentric large Dancer clouds: $a_R \gg a_L$, with $R = 0$.

1. Large $SU(4)$ cloud

The eigenvalues of K are

$$\begin{aligned}
\lambda_1 &= p + q + O(R, a_L, a_R) \\
\lambda_2 &= p + q + O(R, a_L, a_R) \\
\lambda_3 &= p - q + O(R, a_L, a_R) \\
\lambda_4 &= p - q + O(R, a_L, a_R).
\end{aligned} \tag{6.30}$$

Our assumption that $p \pm q \gg R, a_L, a_R$ ensures that these eigenvalues are all positive.

If $r \ll p - q$, the various \hat{V}_a^0 are of order $\sqrt{r_R}$, $\sqrt{r_L}$, $\sqrt{a_R}$, or $\sqrt{a_L}$, depending on whether \mathbf{r} is outside or inside a Dancer cloud. Because these are all small compared to the eigenvalues of K , the second term in Eq. (6.2) can be neglected, $\hat{B} \approx I_4$ and $\hat{\Phi}$ is a composite of two Dancer fields. If instead $r \gg p - q$, then \mathbf{r} is well outside both Dancer clouds and the \hat{V}_a^0 are all insensitive to the SU(2) orientation of the Dancer clouds. We can, therefore, orient the SU(4) cloud parameters so that $\mathbf{q} = (0, 0, q)$ (thus making K diagonal) and at the same time choose

$$\begin{aligned}
\hat{V}_1^0 &\approx \sqrt{2r} \begin{pmatrix} \bar{\psi}(\mathbf{r}) \\ 0 \end{pmatrix} & \hat{V}_2^0 &\approx \sqrt{2r} \begin{pmatrix} 0 \\ \bar{\psi}(\mathbf{r}) \end{pmatrix} \\
\hat{V}_3^0 &\approx \sqrt{2r} \begin{pmatrix} \psi(\mathbf{r}) \\ 0 \end{pmatrix} & \hat{V}_4^0 &\approx \sqrt{2r} \begin{pmatrix} 0 \\ \psi(\mathbf{r}) \end{pmatrix}.
\end{aligned} \tag{6.31}$$

(We have used the fact that $r_L \approx r_R$ in this region.) To leading approximation, this makes \hat{B} diagonal. Since $\hat{\phi}$ is also diagonal outside the Dancer clouds,

$$\hat{\Phi} \approx \frac{1}{2r} \begin{pmatrix} \frac{p-q}{p-q+2r} & 0 & 0 & 0 \\ 0 & \frac{p+q}{p+q+2r} & 0 & 0 \\ 0 & 0 & -\frac{p-q}{p-q+2r} & 0 \\ 0 & 0 & 0 & -\frac{p+q}{p+q+2r} \end{pmatrix}. \tag{6.32}$$

Thus, there are effectively two SU(4) clouds, one at $r \approx p + q$ and one at $r \approx p - q$. In the region outside both clouds, there are no non-Abelian Coulomb magnetic fields. In the intermediate region between the two clouds, the field corresponds to a non-Abelian magnetic charge

$$Q_{NA} = \text{diag}(0, -1, 0, 1). \tag{6.33}$$

In the region inside the inner SU(4) cloud, but still outside the two Dancer clouds, the fields correspond to

$$Q_{NA} = \text{diag}(-1, -1, 1, 1). \tag{6.34}$$

2. Widely separated Dancer clouds

If $R \gg a_L, a_R$, the eigenvalues of K are

$$\begin{aligned}
 \lambda_1 &= p + q + R + O(a_L, a_R) \\
 \lambda_2 &= p + q - R + O(a_L, a_R) \\
 \lambda_3 &= p - q + R + O(a_L, a_R) \\
 \lambda_4 &= p - q - R + O(a_L, a_R).
 \end{aligned} \tag{6.35}$$

In order that these all be positive, $p \pm q \geq R$ [up to $O(a_L, a_R)$ corrections], which implies that $\lambda_1, \lambda_3 \geq 2R$.

If the SU(2) basis is chosen so that $\mathbf{q} = (0, 0, q)$, then, up to $O(a_L, a_R)$ corrections, K is diagonal with

$$K^{-1} = \text{diag} \left(\frac{1}{\lambda_1}, \frac{1}{\lambda_2}, \frac{1}{\lambda_3}, \frac{1}{\lambda_4} \right). \tag{6.36}$$

In the region outside both Dancer clouds ($r_R \gg a_R, r_L \gg a_L$), the SU(2) orientation of the Dancer clouds is irrelevant and we can take

$$\begin{aligned}
 \hat{V}_1^0 &\approx \sqrt{2r_R} \begin{pmatrix} \bar{\psi}(\mathbf{r}_R) \\ 0 \end{pmatrix} & \hat{V}_2^0 &\approx \sqrt{2r_R} \begin{pmatrix} 0 \\ \bar{\psi}(\mathbf{r}_R) \end{pmatrix} \\
 \hat{V}_3^0 &\approx \sqrt{2r_L} \begin{pmatrix} \psi(\mathbf{r}_L) \\ 0 \end{pmatrix} & \hat{V}_4^0 &\approx \sqrt{2r_L} \begin{pmatrix} 0 \\ \psi(\mathbf{r}_L) \end{pmatrix}.
 \end{aligned} \tag{6.37}$$

Examining the factors that enter into \hat{B} , we see that it is composed of two interlocking 2×2 blocks. One (containing the 11-, 13-, 31-, and 33-elements) is of the form of Eq. (4.26) that we encountered in the construction of the SU(4) (1, [1], 1) solution, except that the cloud parameter is now $p + q$. The other (lying in the second and fourth rows and columns) is similar, except with cloud parameter $p - q$.

Now consider the region inside one of the Dancer clouds. Choosing the right cloud, for definiteness, we have $\mathbf{r}_L \approx (0, 0, R)$. The two \hat{V}_a^0 from the right-hand construction problem are

$$\hat{V}_1^0 = O(r_R/\sqrt{a_R}) \quad \hat{V}_2^0 \approx \sqrt{2a_R} \begin{pmatrix} g \\ -f \\ f^* \\ g^* \end{pmatrix} \tag{6.38}$$

where, as in Eq. (5.28), f and g are elements of the SU(2) matrix that relates the $\boldsymbol{\tau}^R$ to the standard set of $\boldsymbol{\tau}$. Since this region is well outside the left Dancer cloud, the SU(2) orientation of that cloud is irrelevant and the remaining \hat{V}_a^0 can be taken to be

$$\begin{aligned}
\hat{V}_3^0 &\approx \sqrt{2R} \begin{pmatrix} \psi(\mathbf{r}_L) \\ 0 \end{pmatrix} \approx \sqrt{2R} \begin{pmatrix} 1 \\ O(a_L/R, a_R/R) \\ 0 \\ 0 \end{pmatrix} \\
\hat{V}_4^0 &\approx \sqrt{2R} \begin{pmatrix} 0 \\ \psi(\mathbf{r}_L) \end{pmatrix} \approx \sqrt{2R} \begin{pmatrix} 0 \\ 0 \\ 1 \\ O(a_L/R, a_R/R) \end{pmatrix}.
\end{aligned} \tag{6.39}$$

We now use the facts that λ_1^{-1} and λ_3^{-1} are at most $O(1/R)$ and that λ_2^{-1} and λ_4^{-1} can be at most $O(1/a_R)$ before our approximations break down. Together with the above expressions for the \hat{V}_a^0 , these imply that all the elements of \hat{B}_{ab} are of order unity or smaller. In fact, the off-diagonal elements are $O(\sqrt{a_R/R})$, except for $\hat{B}_{12} = (\hat{B}_{21})^* = O(r_R/a_R)$. Hence, there is no significant modification of the Dancer Higgs fields inside the Dancer cloud.

The results of this analysis are summarized in Fig. 4, where we indicate the regions delineated by the various clouds and show the value of Q_{NA} in each.

3. Two concentric large Dancer clouds

We now consider two concentric Dancer clouds, with $a_R \equiv a \gg a_L$. Without loss of generality, we can choose the SU(2) orientation of the right Dancer cloud so that the $\boldsymbol{\tau}^R$ are the standard Pauli $\boldsymbol{\tau}$. The orientation of the SU(4) cloud, encoded in \mathbf{q} , and of the left Dancer cloud are arbitrary; the orientation of the latter will actually play no role in our considerations. Finally, because these solutions are spherically symmetric, it is sufficient to examine the fields along the positive z -axis.

The matrix K is

$$K \approx [p\mathbf{I}_2 + \mathbf{q} \cdot \boldsymbol{\tau}] \otimes \mathbf{I}_2 + a_R \tau_i^R \otimes \sigma_i. \tag{6.40}$$

To leading order, its eigenvalues (although not its eigenvectors) are independent of the direction of \mathbf{q} . They are

$$\begin{aligned}
\lambda_1 &= p + q + a + O(a_L) \\
\lambda_2 &= p - a + \sqrt{4a^2 + q^2} + O(a_L) \\
\lambda_3 &= p - q + a + O(a_L) \\
\lambda_4 &= p - a - \sqrt{4a^2 + q^2} + O(a_L).
\end{aligned} \tag{6.41}$$

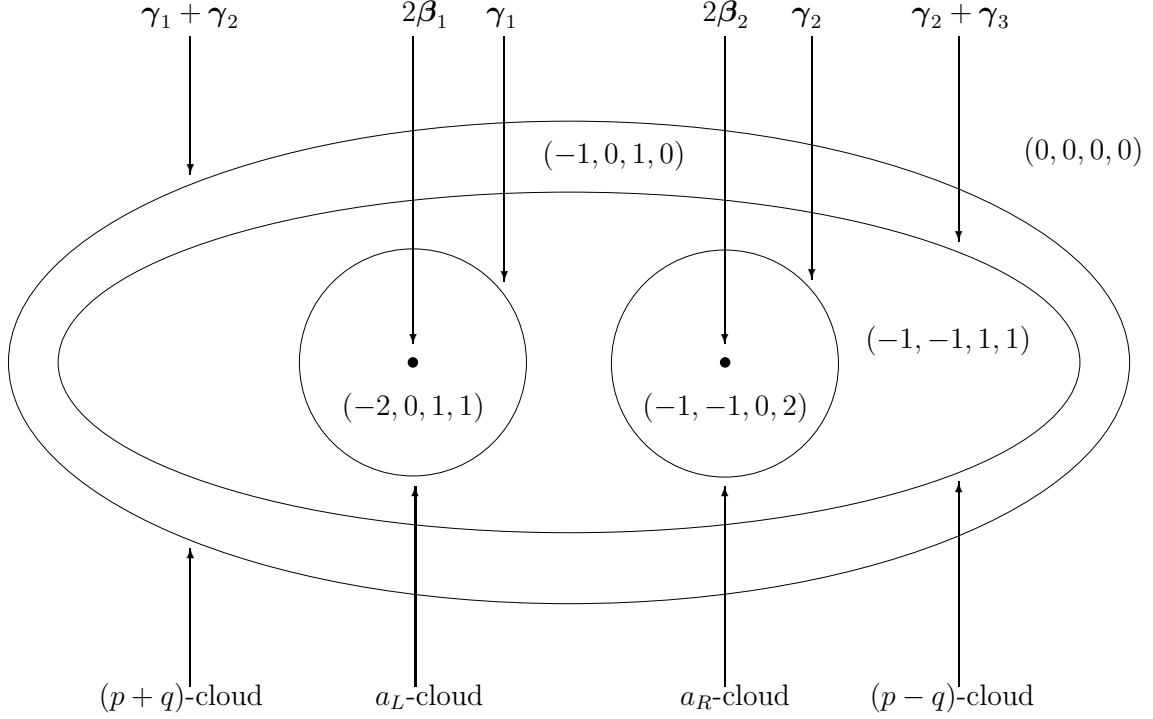


FIG. 4. Schematic illustration of a solution with two widely-separated large Dancer clouds. The clouds are labelled both by the relevant distance scale and by the associated massless monopole. The diagonal elements of Q_{NA} , which is assumed to be a diagonal matrix, are shown for each of the regions defined by the clouds.

These obey $\lambda_1 \geq \lambda_2 \geq \lambda_3 > \lambda_4$, with the first two relations being equalities only if $q = 0$. Note that the last relation can never be an equality, so only λ_4 can vanish. Furthermore, once p is chosen to make λ_4 positive, the remaining λ_j are all $O(a)$ or larger.

We will examine separately the region well outside the Dancer cloud, $r \gg a$, and the region well inside the cloud, $r \ll a$. Outside the cloud, it is possible to choose a basis so that the \hat{V}_j^0 along the z -axis are

$$\begin{aligned}
 \hat{V}_1^0 &= \sqrt{2r} (0, 1, 0, 0)^t \\
 \hat{V}_2^0 &= \sqrt{2r} (0, 0, 0, 1)^t \\
 \hat{V}_3^0 &= \sqrt{2r} (1, 0, 0, 0)^t \\
 \hat{V}_4^0 &= \sqrt{2r} (0, 0, 1, 0)^t.
 \end{aligned} \tag{6.42}$$

In this basis,

$$\hat{\varphi} = \frac{1}{2r} \text{diag}(1, 1, -1, -1). \quad (6.43)$$

There several possibilities to consider, depending on the magnitudes of the λ_j . If these eigenvalues are all $O(a)$ or smaller, then in this region all of the eigenvalues of \hat{B} will be $O(r/a)$ and $\hat{\Phi}$ will be $O(a/r^2)$, corresponding to complete shielding of the non-Abelian magnetic charge. If, instead, the λ_j are all much greater than a , the ‘‘large SU(4) cloud’’ analysis given above applies. There are effectively two SU(4) clouds, one of radius $p + q$ and other of radius $p - q$. The effective non-Abelian magnetic charge vanishes outside both, is given by Eq. (6.33) between the two, and is given by Eq. (6.34) for $p - q \gg r \gg a$.

The only remaining possibility is that $\lambda_1 \approx \lambda_2 \approx p + q \gg a$ while λ_3 and λ_4 are $O(a)$ or smaller. As before, the non-Abelian charge is completely shielded for $r \gg p + q$. In calculating the fields at shorter distance to leading order in a/r , we can approximate K^{-1} by $\Pi K^{-1} \Pi$, where

$$\Pi \approx \frac{\mathbb{I}_2 + \hat{\mathbf{q}} \cdot \boldsymbol{\tau}}{2} \otimes \mathbb{I}_2 \quad (6.44)$$

projects onto the subspace spanned by the eigenvectors corresponding to λ_3 and λ_4 . It is easy to see that by a change of basis that mixes \hat{V}_1^0 with \hat{V}_2^0 and \hat{V}_3^0 with \hat{V}_4^0 one can obtain new vectors such that $\hat{V}'_1{}^0$ and $\hat{V}'_3{}^0$ lie in the subspace onto which Π projects while $\hat{V}'_2{}^0$ and $\hat{V}'_4{}^0$ lie in the orthogonal subspace. (This change of basis leaves Eq. (6.43) unchanged.) In this basis \hat{B} is approximately the identity in the 2-4 subspace, but has two large eigenvalues (of order r/a) in the 1-3 subspace. As a result, two of the eigenvalues of the Higgs field are shielded, so that the only large components are in the 2-4 subspace and the effective magnetic charge is given by Eq. (6.33).

We now turn to the region well inside the Dancer cloud, $r \ll a$, although still with $r \gg a_L$. To leading order in r/a the \hat{V}_j^0 along the positive z -axis can be taken to be

$$\begin{aligned} \hat{V}_1^0 &= \sqrt{2r} (0, 0, 0, 1)^t \\ \hat{V}_2^0 &= \sqrt{2a} (0, -1, 1, 0)^t \\ \hat{V}_3^0 &= \sqrt{2r} (1, 0, 0, 0)^t \\ \hat{V}_4^0 &= \sqrt{2r} (0, 0, 1, 0)^t \end{aligned} \quad (6.45)$$

while to the same order

$$\hat{\varphi} = \frac{1}{2r} \text{diag}(2, 0, -1, -1). \quad (6.46)$$

If all of the λ_j are $O(a)$ or larger, then $\hat{B} \approx I$ in this region and there is no shielding of non-Abelian magnetic charge. The only other possibility is that $\lambda_4 \equiv \Delta \ll a$, with the remaining λ_j being at least $O(a)$. We now examine this second case. Let u be the eigenvector of K with eigenvalue λ_4 , and define $w_j = u^\dagger \hat{V}_j^0$. Using the above expressions for the \hat{V}_j^0 , we have

$$\hat{B}_{ij} = \delta_{ij} + \frac{1}{\Delta} w_i^\dagger w_j + c \delta_{i2} \delta_{j2} + O(\sqrt{r/a}) \quad (6.47)$$

where c is of order unity. Next, note that w_2 is larger than the other w_j by a factor of order $\sqrt{r/a}$ that arises from the relative magnitudes of the \hat{V}_j^0 . Hence, to leading order the term containing c can be included in the $w_i^\dagger w_j$ term, giving

$$\hat{B}_{ij} = \delta_{ij} + \frac{(1+c\Delta)}{\Delta} w_i^\dagger w_j + O(\sqrt{r/a}). \quad (6.48)$$

Inverting this matrix gives

$$\begin{aligned} (\hat{B}^{-1})_{ij} &= \delta_{ij} - \frac{w_i^\dagger w_j}{|w|^2} + \frac{\Delta w_i^\dagger w_j}{(1+c\Delta)|w|^4} + O(\sqrt{r/a}) \\ &= \delta_{ij} - \delta_{i2} \delta_{j2} + O(\sqrt{r/a}) \end{aligned} \quad (6.49)$$

where $|w|^2 = w_i^\dagger w_i$. Recalling the vanishing of $\hat{\varphi}_{22}$ in Eq. (6.46), we see that to leading order in r/a there is no modification of the Higgs field.

It is straightforward to extend this analysis to the region, $r \ll a_L$, inside the smaller cloud and to show that to leading order the SU(4) clouds do not modify the Higgs field there. This result does not depend on the relative SU(2) orientation of the two Dancer clouds.

To summarize, we can distinguish five concentric regions (four, if $p - q \sim a_R$). The effective magnetic charges seen within these are

$$Q_{NA} = \begin{cases} \text{diag}(0, 0, 0, 0), & r \gg p + q \\ \text{diag}(0, -1, 0, 1), & p + q \gg r \gg \text{Max}(p - q, a_R) \\ \text{diag}(-1, -1, 1, 1), & p - q \gg r \gg a_R \\ \text{diag}(-2, 0, 1, 1), & a_R \gg r \gg a_L \\ \text{diag}(-2, 0, 0, 2), & a_L \gg r \end{cases} \quad (6.50)$$

We illustrate this in Fig. 5.

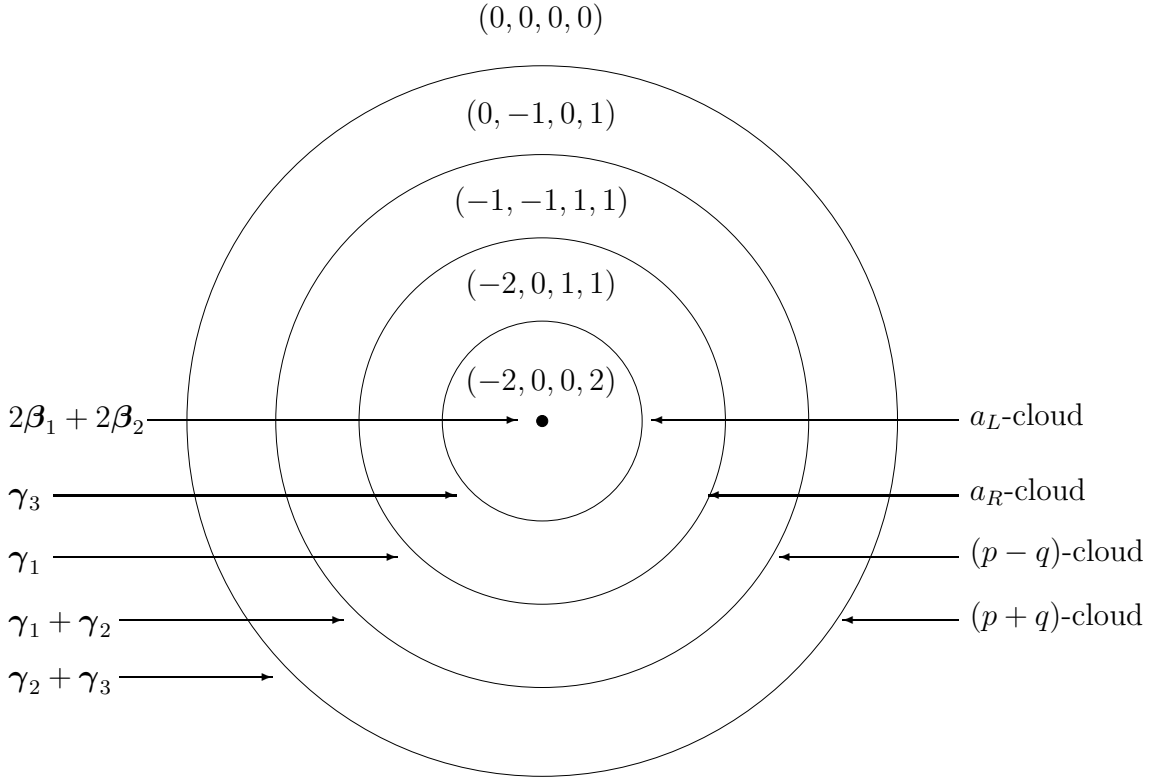


FIG. 5. Schematic illustration of a solution with two concentric large Dancer clouds. The clouds are labelled both by the relevant distance scale and by the associated massless monopole. The diagonal elements of Q_{NA} , which is assumed to be a diagonal matrix, are shown for each of the regions defined by the clouds.

VII. CLOUDS AND MASSLESS MONOPOLES

With the explicit examples of the previous section in hand, we can now examine more closely the relationship between the massless monopoles and the non-Abelian clouds. The first thing to notice is that there are six massless monopoles but only four non-Abelian clouds. In other words, the number of distinct clouds evident in the solutions is less than the number of massless monopoles obtained by adding the coefficients of the γ_a in Eq. (1.4).⁵ The number of degrees of freedom in the $SU(6)$ $(2, [2], [2], [2], 2)$ solutions, 40, is precisely

⁵This is not a completely new phenomenon; the $SU(N)$ $(1, [1], \dots, [1], 1)$ solutions have $N - 3$ massless monopoles but only a single cloud. However, these might have been dismissed as special cases because they can all be obtained as embeddings of $(1, [1], 1)$ $SU(4)$ solutions with a single massless monopole.

that expected when there are a total of ten (four massive and six massless) monopoles. However, in all the examples we have studied, these degrees of freedom parameterize the four massive monopoles and only four distinct, though sometimes degenerate, clouds. In other words, there is not a one-to-one correspondence between clouds and massless monopoles. We expect that the solutions we have studied are not exceptional in this regard and that a general $(2, [2], [2], [2], 2)$ will have four clouds.

To help understand this, recall that requiring that $\mathbf{h} \cdot \boldsymbol{\beta}_a$ is positive determines a unique set of simple roots when the symmetry is maximally broken, but when the unbroken group has a non-Abelian factor $\mathbf{h} \cdot \boldsymbol{\beta}_a = 0$ for some $\boldsymbol{\beta}_a$'s and so there are a number of possible choices for the simple roots, all related by Weyl transformations. To be specific, let us consider $SU(6)$. Following Fig. 1, we denote the simple roots for the maximally broken case by $\boldsymbol{\beta}_1$, $\boldsymbol{\gamma}_1$, $\boldsymbol{\gamma}_2$, $\boldsymbol{\gamma}_3$, and $\boldsymbol{\beta}_2$. Each of these corresponds to a massive fundamental monopole. In the limit where the unbroken symmetry is enlarged to $U(1) \times SU(4) \times U(1)$, the $\boldsymbol{\beta}_1$ -monopole becomes part of a multiplet of degenerate states transforming as a $\mathbf{4}$ of $SU(4)$; the remaining states in this multiplet correspond to the roots $(\boldsymbol{\beta}_1 + \boldsymbol{\gamma}_1)$, $(\boldsymbol{\beta}_1 + \boldsymbol{\gamma}_1 + \boldsymbol{\gamma}_2)$, and $(\boldsymbol{\beta}_1 + \boldsymbol{\gamma}_1 + \boldsymbol{\gamma}_2 + \boldsymbol{\gamma}_3)$, all of which can be obtained from $\boldsymbol{\beta}_1$ by Weyl transformations. Similarly, the $\boldsymbol{\beta}_2$ -monopole is part of a $\bar{\mathbf{4}}$ that also includes the $(\boldsymbol{\beta}_2 + \boldsymbol{\gamma}_3)$ -, $(\boldsymbol{\beta}_2 + \boldsymbol{\gamma}_3 + \boldsymbol{\gamma}_2)$ -, and $(\boldsymbol{\beta}_2 + \boldsymbol{\gamma}_3 + \boldsymbol{\gamma}_2 + \boldsymbol{\gamma}_1)$ -monopoles. Clearly, the straightforward correspondence of simple roots with elementary monopoles and composite roots with multimono poles has become more complicated.

It is useful to make a detailed correspondence between the clouds and the massless monopoles in specific solutions. This can be done by noting the effect of each cloud on the non-Abelian charge Q_{NA} . Recall that the non-Abelian charges of the massive $\boldsymbol{\beta}_1$ - and $\boldsymbol{\beta}_2$ -monopoles are

$$\begin{aligned} Q_{NA}(\boldsymbol{\beta}_1) &= \text{diag}(-1, 0, 0, 0) \\ Q_{NA}(\boldsymbol{\beta}_2) &= \text{diag}(0, 0, 0, 1) \end{aligned} \tag{7.1}$$

while those of the massless monopoles are

$$\begin{aligned} Q_{NA}(\boldsymbol{\gamma}_1) &= \text{diag}(1, -1, 0, 0) \\ Q_{NA}(\boldsymbol{\gamma}_2) &= \text{diag}(0, 1, -1, 0) \\ Q_{NA}(\boldsymbol{\gamma}_3) &= \text{diag}(0, 0, 1, -1) \\ Q_{NA}(\boldsymbol{\gamma}_1 + \boldsymbol{\gamma}_2) &= \text{diag}(1, 0, -1, 0) \\ Q_{NA}(\boldsymbol{\gamma}_2 + \boldsymbol{\gamma}_3) &= \text{diag}(0, 1, 0, -1) \\ Q_{NA}(\boldsymbol{\gamma}_1 + \boldsymbol{\gamma}_2 + \boldsymbol{\gamma}_3) &= \text{diag}(1, 0, 0, -1) \end{aligned} \tag{7.2}$$

where we have listed the charges for all of the massless positive roots, not just the $\boldsymbol{\gamma}_a$.

As an example, consider the case of concentric Dancer clouds illustrated in Fig. 5 and described by Eq. (6.50). In the innermost region, $r \ll a_L$, we have the field due to two $\boldsymbol{\beta}_1$ -

and two β_2 -monopoles. Moving outward, we find a γ_3 -monopole at $r \approx a_L$, a γ_1 -monopole at $r \approx a_R$, a $(\gamma_1 + \gamma_2)$ -monopole at $r \approx p - q$ and finally a $(\gamma_2 + \gamma_3)$ -monopole at $r \approx p + q$.

The fact that two of these roots are simple and two are composite is a gauge-dependent statement; the sequence $\gamma_3, \gamma_1, \gamma_2, (\gamma_1 + \gamma_2 + \gamma_3)$, for example, leads to a physically equivalent configuration. However, the sum of these roots, $2\gamma_1 + 2\gamma_2 + 2\gamma_3$, (corresponding to a total of six massless monopoles) is invariant, as is the fact that two of the roots are ‘‘Dancer roots’’ that are orthogonal to one β_a but not to the other. We can also apply a gauge transformation that replaces one of the β_a by a compound root. Such a transformation will replace some of the positive roots in the above sequences by a negative roots, but the sum of the coefficients of the γ_a will remain unchanged. The correspondence between monopoles and clouds for various solutions is indicated in Figs. 2-5.

Let us try to develop some rules to explain how and where the various massless monopoles can appear in these solutions. It is useful to begin by discussing what happens to the γ_a -monopoles in the maximally broken theory when the Higgs expectation value Φ_0 is varied. As Φ_0 approaches a value with an enlarged symmetry group, the masses of some of the elementary bosons decrease, eventually vanishing in the limit where the symmetry becomes non-Abelian. For an isolated γ_a -monopole, the core radius is inversely proportional to the corresponding elementary boson mass and so grows monotonically and becomes infinite in the non-Abelian limit. Similarly, for a configuration composed of two monopoles, a γ_1 -monopole and a γ_2 -monopole, for example, the component monopoles each grow without bound as the corresponding masses vanish. When their core radii are much larger than the separation of their centers, the two-monopole configuration is barely distinguishable from a gauge-transformed one-monopole solution.

However, the situation can be different if the configuration contains a monopole that remains massive in the non-Abelian limit. If the fields in the massive core transform under the non-Abelian symmetry, some of the massless gauge fields acquire an effective mass near the massive core. This can dramatically modify the behavior of the massless monopole cores. There are three possible situations. One possibility is that the massive and massless monopoles lie in mutually commuting subgroups. The massive monopole then has no effect on the massless monopole, and the behavior described in the previous paragraph is unchanged. Another possibility is that the addition of the massless monopole to the massive monopole corresponds to a gauge transformation of the massive monopole, in which case no gauge-invariant evidence of the massless monopole survives in the non-Abelian limit. The most interesting case is when neither of these holds. The massless monopole core then expands only until it reaches the massive monopole, resulting in a cloud whose radius is equal

to the original intermonopole separation.⁶

A similar pattern should be expected when several massive monopoles are present. A massless monopole with non-Abelian charge q should be able to form a finite size cloud enclosing a collection of monopoles with total charge Q_{NA} only if (1) q does not lie in the subgroup that leaves Q_{NA} invariant and (2) $Q'_{NA} = Q_{NA} + q$ is not gauge-equivalent to Q_{NA} . This is consistent with the behavior of the clouds in both the SU(3) Dancer and the SU(4) $(1, [1], 1)$ solutions. In each case, combining the massless monopole with just one of the massive monopoles would simply give a gauge-transformed massive monopole and, indeed, we only find solutions where the cloud encloses both of the massive monopoles.⁷

Let us apply these rules to the concentric Dancer cloud solutions of Sec. VI B 3. We start with two β_1 - and two β_2 -monopoles, with a total non-Abelian charge

$$Q_1 = 2Q_{NA}(\beta_1) + 2Q_{NA}(\beta_2) = \text{diag}(-2, 0, 0, 2), \quad (7.3)$$

and want to add one of the massless monopoles whose charges were enumerated in Eq. (7.2). There are four possibilities: we can add a massless monopole corresponding to:

- a) γ_1 or $(\gamma_1 + \gamma_2)$; these give gauge-equivalent solutions in the Q_1 background.
- b) γ_3 or $(\gamma_2 + \gamma_3)$; these are similarly gauge-equivalent.
- c) γ_2 .
- d) $(\gamma_1 + \gamma_2 + \gamma_3)$.

Cases (a) and (b) differ only by the interchange of the left and right Dancer solutions, and need not be considered separately. Case (c) is ruled out because γ_2 lies in the SU(2) subgroup that leaves Eq. (7.3) invariant. Thus, it is sufficient to consider cases (b) and (d). We start with the former, and add a γ_3 -monopole to get

$$Q_2 = Q_1 + Q_{NA}(\gamma_3) = \text{diag}(-2, 0, 1, 1). \quad (7.4)$$

The possible choices for the next massless monopole are:

- a) γ_1 .

⁶For a detailed study of how the non-Abelian limit is approached in the last two cases, see Ref. [25].

⁷The minimal cloud solutions can be viewed as having the massless monopole exactly coincident with one of the massive monopoles. However, these should be understood as a limiting case in which the ellipsoidal cloud enclosing the two massive monopoles has degenerated into a line.

- b) $(\gamma_1 + \gamma_2)$ or $(\gamma_1 + \gamma_2 + \gamma_3)$; these are gauge-equivalent to each other.
- c) γ_3 ; this is ruled out because it lies in the $SU(2)$ symmetry group of Eq. (7.4).
- d) γ_2 or $(\gamma_2 + \gamma_3)$; these just gauge transform Q_2 , [e.g., $Q_2 + Q_{NA}(\gamma_2) = \text{diag}(-2, 1, 0, 1)$] and so cannot give rise to a cloud.

Once more, we have two acceptable choices, (a) and (b). If we take the former, we obtain

$$Q_3 = Q_2 + Q_{NA}(\gamma_1) = \text{diag}(-1, -1, 1, 1). \quad (7.5)$$

We cannot add either a γ_1 - or a γ_3 -monopole to this, since both lie in the $SU(2) \times SU(2)$ symmetry group of Q_3 . The remaining four possibilities are all gauge-equivalent. Choosing $(\gamma_1 + \gamma_2)$, we obtain

$$Q_4 = Q_3 + Q_{NA}(\gamma_1 + \gamma_2) = \text{diag}(0, -1, 0, 1). \quad (7.6)$$

At this point, the remaining massless monopoles only allow three possibilities: γ_2 , γ_3 , and $(\gamma_2 + \gamma_3)$. The first two are excluded because they give gauge transforms of Q_4 . The third gives

$$Q_5 = Q_4 + Q_{NA}(\gamma_2 + \gamma_3) = \text{diag}(0, 0, 0, 0). \quad (7.7)$$

We therefore recover the sequence $\gamma_3, \gamma_1, (\gamma_1 + \gamma_2), (\gamma_2 + \gamma_3)$ that we found previously.

We now must return to the alternatives that we did not follow. At the first step, we could have taken case (d) and added a $(\gamma_1 + \gamma_2 + \gamma_3)$ -monopole to Q_1 , thus reaching in one step a charge that was gauge-equivalent to Q_4 . This can be viewed as simply a degenerate case of the four-step sequence, corresponding to the situation where $a_L = a_R = p - q$. The other place where we had an option was in adding on to Q_2 , where we could have followed case (b) and added a $(\gamma_1 + \gamma_2)$ -monopole. Once again, this is simply a degenerate case, equivalent to taking $a_R = p - q$.

Another instructive example is the solution with two minimal Dancer clouds that was analyzed in Sec. VI A 1 and illustrated in Fig. 2. The two β_1 -monopoles “anchor” a massless monopole corresponding (by a gauge choice) to $(\gamma_1 + \gamma_2)$. In this solution the corresponding ellipsoidal Dancer cloud has degenerated into a line, and the fields are those appropriate to two massive monopoles, one with non-Abelian charge

$$Q_{NA}(\beta_1) = \text{diag}(-1, 0, 0, 0) \quad (7.8)$$

at \mathbf{x}_1 , and one with

$$Q_{NA}(\beta_1 + \gamma_1 + \gamma_2) = \text{diag}(0, 0, -1, 0) \quad (7.9)$$

at \mathbf{x}_2 .⁸ Similarly, a $(\gamma_2 + \gamma_3)$ -monopole forms a minimal Dancer cloud about the β_2 -monopoles, effectively yielding a pair of massive monopoles with charges $\text{diag}(0, 1, 0, 0)$ (at \mathbf{x}_3) and $\text{diag}(0, 0, 0, 1)$ (at \mathbf{x}_4). At this point we are left with only two massless monopoles, a γ_1 and a γ_3 . The former can form a cloud anchored by the monopoles at \mathbf{x}_1 and \mathbf{x}_3 , whose total charge is $\text{diag}(-1, 1, 0, 0) = -Q_{\text{NA}}(\gamma_1)$. It could not, on the other hand, have formed a cloud about the \mathbf{x}_1 - and \mathbf{x}_4 - or the \mathbf{x}_2 - and \mathbf{x}_3 -monopoles, because in each case the effect of the γ_1 -monopole would have only been to gauge transform the sum of the charges of the two massive monopoles. By similar arguments, the γ_3 -monopole can only condense about the monopoles at \mathbf{x}_2 and \mathbf{x}_4 .

Similar analyses can be applied to the other limiting cases studied in Sec. VI. In all cases, the appearance of the massless monopoles and their clouds is consistent with the rules outlined above.

VIII. SUMMARY AND CONCLUDING REMARKS

Our goal in this paper has been to gain further insight into the massless monopoles that can arise when a gauge theory is spontaneously broken to a subgroup containing a non-Abelian factor. These can be viewed as limiting cases of massive fundamental monopoles of the maximally broken theory, in the sense that they have the same number of degrees of freedom and that the moduli space metric describing their dynamics is a smooth limit of that for the maximally broken case. In contrast to the massive fundamental monopoles, however, they cannot be realized as isolated classical solutions. Instead, they are manifested through non-Abelian clouds surrounding one or more massive monopoles. We have focussed on the $(2, [2], \dots, [2], 2)$ solutions of $SU(N)$ broken to $U(1) \times SU(N-2) \times U(1)$. These solutions display a much richer structure than the one-cloud solutions that have been previously studied. The case of $N = 6$ is generic, in the sense that the solutions for $N > 6$ can all be obtained by embedding the $SU(6)$ solution; we will discuss the restriction to smaller groups, and in particular $SU(4)$, below.

We have used the Nahm construction to obtain these solutions. A crucial ingredient in the application of this construction is the fact that the Nahm data for the $SU(6)$ problem are equivalent to two sets of $SU(3)$ Dancer Nahm data, together with a set of constant jump

⁸It seems obvious here that the $(\gamma_1 + \gamma_2)$ -monopole is coincident with one of the massive monopoles. Nevertheless, the position of this massless monopole, as defined by the boundary values of 22-components of the Nahm data, can, by an appropriate change of basis, be taken to be any point along the line joining the two β_1 -monopoles. A similar phenomenon occurs in the minimal cloud $(1, [1], 1)$ solutions in $SU(4)$.

data. In the particular case where the jump data are large compared to the other scales in the problem, they define a pair of nested “SU(4) clouds” that enclose two independent Dancer solutions, characterized by Dancer cloud parameters a_L and a_R .

The spacetime fields of the SU(6) solution can be obtained from those of the related Dancer solutions by purely algebraic manipulations. Although the Dancer fields are not explicitly known for arbitrary parameters, analytic approximations can be obtained both in the limit where a is much greater than the separation of the massive monopoles and in the case of minimal Dancer cloud. Using these approximations, we have obtained the leading behavior of the SU(6) solutions for a number of limiting cases.

In these solutions, the clouds divide space into distinct regions, each of which can be characterized by a non-Abelian magnetic charge Q_{NA} . By comparing the values of Q_{NA} in adjacent regions, one can establish a correspondence between a specific cloud and a particular massless monopole. In each case, one or more clouds are associated with massless monopoles corresponding to compound, rather than simple, roots. As a result, the number of fundamental massless monopoles (as defined, e.g., by the counting of degrees of freedom), which is obtained by adding the coefficients of the simple roots in Eq. (1.4), is greater than the number of distinct clouds. The SU(6) solutions contain six massless monopoles but only four clouds, of which two are inherited from the Dancer solutions and two are SU(4) clouds associated with the jump data.

Our explicit solutions also help clarify the role of the parameters that enter the general $(2, [2], [2], [2], 2)$ solution. The moduli space is 40-dimensional, with 17 of these corresponding to the unbroken $U(1) \times SU(4) \times U(1)$ symmetry. The remaining 23 parameters were enumerated at the end of Sec. III. Twelve of these specify the positions of the massive monopoles, and two others give the relative U(1) phase between pairs of identical massive monopoles. As with the U(1) phase parameter in the SU(2) two-monopole solution, the effect of these phases falls exponentially with the monopole separation. They have, therefore, played no role in our analysis, which focussed on the region outside of the massive monopole cores.

The remaining nine parameters are associated with the non-Abelian clouds. Roughly speaking, four of these (a_L , a_R , p , and q) are cloud size parameters and five determine the relative SU(2) orientations of the Dancer and SU(4) clouds. However, as the example of Sec. VIA 2 shows, this division between size and orientation parameters is not completely clearcut, since the shape of the cloud can depend upon the orientation parameters.

It is instructive to compare the SU(2) orientation parameters with the U(1) phase parameters. The latter would be true symmetry parameters, having no effect on the form of the solutions, were it not for the interactions between the U(1)-charged fields in the cores of the massive monopoles. The exponential falloff in the effect of these parameters results

from the fact that fields with U(1) charge are all massive. The role of the SU(2) parameters is similar, but because there are massless fields carrying SU(2) charges, the effect of these parameters only falls as a power of distance. Note that the distance to the SU(4) cloud is crucial here, since the Dancer solutions lie in mutually commuting subgroups and therefore have no direct interactions.

It is also useful to consider the application of our results to smaller groups. In particular, let us try to identify those SU(6) solutions that can be viewed as embeddings of the $(2, [2], 2)$ SU(4) solutions. In the Nahm construction, these are distinguished by the fact that their jump data includes only two independent a_p , rather than four. In terms of the construction of Sec. IV, this translates into the statement that two of the eigenvalues of K vanish. A more physical characterization is based on the fact that the SU(4) solutions contain only two massless monopoles, and thus, at most, two distinct clouds. Hence, they must correspond to SU(6) solutions in which some of the clouds are coincident.

Let us apply these considerations to some of the examples discussed in Sec. VI:

1. *Minimal Dancer clouds with all SU(2)'s aligned* (Sec. VIA 1): There are two ways for K to have two vanishing eigenvalues. One is to set $p + q = |\mathbf{x}_1 - \mathbf{x}_3|$ and $p - q = |\mathbf{x}_2 - \mathbf{x}_4|$. This is equivalent to a pair of SU(4) $(1, [1], 1)$, each of which has a minimal cloud and is thus an SU(3) solution embedded in SU(4). The alternative is to take $p = q$ and $\mathbf{x}_2 = \mathbf{x}_4$. This is equivalent to an SU(4) $(1, [1], 1)$ solution, with massive monopoles at \mathbf{x}_1 and \mathbf{x}_3 and cloud size $p + q = 2p$, together with a minimal cloud SU(4) $(1, [1], 1)$ solution with coincident massive monopoles at \mathbf{x}_2 .

2. *Minimal Dancer clouds with coincident massive monopoles* (Sec. VIA 2): Equation (6.11) shows that two eigenvalues of K vanish if $p = q$. Equation (6.12) then implies that the nonvanishing components of the Higgs field must lie in the subspace orthogonal to M^- . If the angle α defined in Eq. (6.15) vanishes, this gives the second solution of case (1), but with the restriction that $\mathbf{x}_1 = \mathbf{x}_3$. On the other hand, if $\alpha \neq 0$, corresponding to misaligned SU(2) orientations, then the outermost cloud (specified roughly by $\lambda_+ = 1$) encloses all four of the massive monopoles.

3. *Two widely separated large Dancer clouds* (Sec. VIB 2): The vanishing of two of the eigenvalues in Eq. (6.35) implies that $p = R + O(a)$ and $q = O(a)$; a more careful analysis of Eq. (6.29) is needed to determine the exact values. This leads to a somewhat degenerate version of the situation depicted in Fig. 4, with the two Dancer clouds and the two SU(4) clouds not clearly distinguishable.

4. *Two concentric large Dancer clouds* (Sec. VIB 3): If we insist that $a_R \gg a_L$, as in our previous analysis, then at most one eigenvalue of K can vanish, implying that this cannot be reduced to an SU(4) solution. On the other hand, examination of Eq. (6.29) suggests

that there should be embedded SU(4) solutions with $a_R \approx a_L \approx p - q$. In terms of the discussion following Eq. (7.6), this corresponds to having the clouds from the γ_1 -, the γ_3 -, and the $(\gamma_1 + \gamma_2)$ -monopoles all coincident, with the fourth, $(\gamma_2 + \gamma_3)$, cloud at a (possibly much larger) radius $p + q$.

For SU(4) broken to $U(1) \times SU(2) \times U(1)$, a solution containing k_1 β_1 -monopoles and k_2 β_2 -monopoles has vanishing SU(2) magnetic charge, and thus no asymptotic non-Abelian Coulomb field, if there are exactly $(k_1 + k_2)/2$ massless γ -monopoles. However, this tells us little about the magnetic field at finite distances. In particular, we would like to know whether the massive monopoles are “paired up” to form SU(2)-neutral combinations composed of two massive monopoles enclosed by a single massless monopole cloud. It is certainly clear that configurations of this sort must exist. Thus, there should be $(2, [2], 2)$ solutions that are approximately the sum of two widely separated $(1, [1], 1)$ solutions, as well as others that correspond to two widely separated Dancer solutions, one formed from the β_1 -monopoles and one from the β_2 -monopoles. The question is whether this is the generic situation. The solutions described in paragraph (2) are instructive in this regard. For $\alpha = 0$ these do, indeed, naturally separate into a pair of $(1, [1], 1)$ solutions. However, for the presumably more generic case of nonzero α , we find that the “ λ_+ -cloud” encloses all four massive monopoles. This strongly suggests that in general there is no clear pairing of massive monopoles.

Finally, we want to indicate briefly two areas for future research. The first is the determination of the $(2, [2], \dots, [2], 2)$ moduli space metric, which determines the low-energy dynamics of the monopoles. In general, the explicit determination of such metrics is a difficult task. However, one might hope that relation between the Dancer Nahm data and the $(2, [2], \dots, [2], 2)$ Nahm data could be exploited to allow a construction of the moduli space metric in terms of the Dancer metric [11]. Secondly, one would like to understand better the quantum theory of monopoles with non-Abelian charges, and in particular the complex interplay of the non-Abelian electric and magnetic charges [26]. The knowledge of classical multicloud solutions that we have gained should help provide a starting point for this investigation.

ACKNOWLEDGMENTS

This work was supported in part by the U.S. Department of Energy. CJH is grateful to the Fulbright Commission and to the Royal Commission for the Exhibition of 1851 for financial support and to the Department of Physics, Columbia University for hospitality.

REFERENCES

- [1] C. Montonen and D. I. Olive, Phys. Lett. B **72**, 117 (1977).
- [2] K. Lee, E. J. Weinberg, and P. Yi, Phys. Rev. D **54**, 6351 (1996).
- [3] E. B. Bogomolny, Sov. J. Nucl. Phys. **24**, 449 (1976) [Yad. Fiz. **24**, 861 (1976)].
- [4] M. K. Prasad and C. M. Sommerfield, Phys. Rev. Lett. **35**, 760 (1975).
- [5] F. Englert and P. Windey, Phys. Rev. D **14**, 2728 (1976); P. Goddard, J. Nuyts, and D. I. Olive, Nucl. Phys. B **125**, 1 (1977).
- [6] E. J. Weinberg, Nucl. Phys. B **167**, 500 (1980).
- [7] A. Abouelsaood, Phys. Lett. B **125**, 467 (1983); P. Nelson and A. Manohar, Phys. Rev. Lett. **50**, 943 (1983); A. P. Balachandran, G. Marmo, N. Mukunda, J. S. Nilsson, E. C. Sudarshan, and F. Zaccaria, Phys. Rev. Lett. **50**, 1553 (1983); P. Nelson and S. R. Coleman, Nucl. Phys. B **237**, 1 (1984).
- [8] E. J. Weinberg, Nucl. Phys. B **203**, 445 (1982).
- [9] E. J. Weinberg, Phys. Lett. B **119**, 151 (1982).
- [10] E. J. Weinberg and P. Yi, Phys. Rev. D **58**, 046001 (1998).
- [11] A. S. Dancer, Commun. Math. Phys. **158**, 545 (1993).
- [12] A. S. Dancer, Nonlinearity **5**, 1355 (1992).
- [13] K. Lee and C. Lu, Phys. Rev. D **57**, 5260 (1998).
- [14] C. J. Houghton, Phys. Rev. D **56**, 1220 (1997).
- [15] C. J. Houghton, P. W. Irwin, and A. J. Mountain, JHEP **9904**, 029 (1999).
- [16] W. Nahm, in *Monopoles in quantum field theory*, Craigie et al. eds. (World Scientific, Singapore, 1982); in *Gauge theories and lepton hadron interactions*, edited by Z. Horvath et al. (Central Research Institute for Physics, Budapest, 1982); in *Structural Elements in Particle Physics and Statistical Mechanics*, edited by J. Honerkamp et al. (Plenum, New York, 1983) in *Group theoretical methods in physics*, Denardo et al. eds. (Springer-Verlag, 1984).
- [17] M. F. Atiyah, N. J. Hitchin, V. G. Drinfeld, and Y. I. Manin, Phys. Lett. A **65**, 185 (1978).
- [18] N. J. Hitchin, Commun. Math. Phys. **89**, 145 (1983).
- [19] E. Corrigan and P. Goddard, Annals Phys. **154**, 253 (1984).
- [20] W. Nahm, Phys. Lett. B **90**, 413 (1980).
- [21] J. Hurtubise and M. K. Murray, Commun. Math. Phys. **122**, 35 (1989).
- [22] A. S. Dancer and R. A. Leese, Phys. Lett. B **390**, 252 (1997).
- [23] P. Irwin, Phys. Rev. D **56**, 5200 (1997).
- [24] A. S. Dancer and R. A. Leese, Proc. R. Soc. Lond. A **440**, 421 (1993).
- [25] C. Lu, Phys. Rev. D **58**, 125010 (1998).

- [26] F. A. Bais and B. J. Schroers, Nucl. Phys. B **512**, 250 (1998); B. J. Schroers and F. A. Bais, Nucl. Phys. B **535**, 197 (1998).